EXPERIMENTAL CELL RESEARCH 330 (2015) 135–150

Available online at www.sciencedirect.com

ScienceDirect

journal homepage: www.elsevier.com/locate/yexcr

Research Article

Dedifferentiation of cancer cells following recovery from a potentially lethal damage is mediated by H_2S–Nampt

Elena A. Ostrakhovitch[a], *Shin Akakura*[a], *Reiko Sanokawa-Akakura*[a], *Scott Goodwin*[b], *Siamak Tabibzadeh*[a,b,*]

[a]*Frontiers in Bioscience Research Institute in Aging and Cancer, Irvine, CA 92618, USA*
[b]*Department of Radiological Sciences, University of California, Irvine, CA 92868, USA*

ARTICLE INFORMATION

Article Chronology:
Received 1 June 2014
Received in revised form
18 September 2014
Accepted 20 September 2014
Available online 30 September 2014

Keywords:
Hydrogen sulfide
Nampt
Cancer cells
Potentially lethal damage recovery
Dedifferentiation

ABSTRACT

Recently, we reported that cancer cells that recover from a potentially lethal damage gain new phenotypic features comprised of mitochondrial structural remodeling associated with increased glycolytic dependency and drug resistance. Here, we demonstrate that a subset of cancer cells, upon recovery from a potentially lethal damage, undergo dedifferentiation and express genes, which are characteristic of undifferentiated stem cells. While these cells are competent in maintaining differentiated progeny of tumor, they also exhibit transdifferentiation potential. Dedifferentiation is characterized by accumulation of hydrogen sulfide (H_2S), which triggers up-regulation of nicotinamide phosphoribosyltransferase (Nampt) accompanied by changes in the redox state. The molecular events triggered by Nampt include elevated production of NAD^+ and up-regulation of H_2S producing enzymes, cystathionine beta synthase (CBS) and cystathionase (CTH) with 3-mercaptopyruvate sulfurtransferase (MST) being detectable only in 3D spheroids. Suppression of Nampt, or inactivation of H_2S producing enzymes, all reduce H_2S production and reverse the ability of cells to dedifferentiate. Moreover, H_2S induced stem cell markers in parental cancer cells in a manner similar to that observed in damage recovered cells. These data suggest of existence of a positive feedback loop between H_2S and Nampt that controls dedifferentiation in cancer cells that recover from a potentially lethal damage.

© 2014 The Authors. Published by Elsevier Inc. This is an open access article under the CC BY-NC-ND license (http://creativecommons.org/licenses/by-nc-nd/3.0/).

Abbreviations: CBS, Cyctathionine beta synthase; CTH, Cystathionase; MST, 3-mercaptopyruvate sulfurtransferase; PLDR, potentially lethal damage recovery; CHH, O-(carboxymethyl) hydroxylamine hemihydrochloride, inhibitor of Cyctathionine beta synthase; PAG, DL-propargylglycine, inhibitor of cystathione gamma-lyase; DR^{G-}, Glucose deprivation induced DR cells; DR^{H2O2}, Hydrogen peroxide induced DR cells; DR^{H}, Hypoxia induced DR cells; NAD^+, Nicotinamide adenine dinucleotide; Nampt, Nicotinamide phosphoribosyltransferase; Pc, Parental control tumor cells; DR, Damage-recovered cells; SEM, Standard error of the mean; Sp, spheroidal colonies; T^v, Viable tumor derived cells isolated within the first 24 h from in vivo generated tumors

*Corresponding author at: Frontiers in Bioscience Research Institute in Aging and Cancer, 16471 Scientific Way, Irvine, CA 92618 USA.
E-mail address: fbs@bioscience.org (S. Tabibzadeh).

http://dx.doi.org/10.1016/j.yexcr.2014.09.027
0014-4827/© 2014 The Authors. Published by Elsevier Inc. This is an open access article under the CC BY-NC-ND license (http://creativecommons.org/licenses/by-nc-nd/3.0/).

Introduction

In the past few years, the idea that cancers arise, progress, and initiate new tumors from a small number of cells with the capability of infinite self-renewal and which harbor the potential to differentiate has got a great momentum [1]. It is now recognized that the molecular signature of such cells is similar to that of embryonic stem cells (ESC). The expression of key factors that control stem cell identity such as *OCT4* has been reported in a variety of cancers including hepatocellular, gastric and cervical carcinomas [2–4]. It has been suggested that *OCT4*$^+$ cancer cells might be tumor-initiating stem cells, a concept that is consistent with the role of this transcription factor in the maintenance of stem cell pluripotency. However, the presence of embryonic *OCT4A* in tumor tissue and tumor cell lines was doubted by some who attributed the observed *OCT4* expression to the expression of *OCT4* pseudogene [5–6]. On the other hand, the expression of another important member of the pluripotency regulatory network *SOX2* (Sex-determining region Y (SRY)-Box2) was also reported in various cancers and cancer cell lines [7–9]. It has been suggested that *SOX2* contributes to the dedifferentiation of cancer cells, endowing them with highly aggressive properties [7,10]. *OCT4* and *SOX2* cooperatively stimulate the transcription of several downstream target genes such as *NANOG*, *DPPA2* (developmental pluripotency-associated two), and *FBXO15*, which also show oncogenic transformation activity [11–13].

The stem cell theory of cancer proposes two major concepts. The first concept suggests that cancers arise from malignant stem cells that are present in somatic tissues, whereas the second concept stresses the importance of dedifferentiation of somatic cells due to factors in their microenvironment [14–16]. However, the origin of cancer stem cells remains the subject of an intense ongoing research; whether such cells give rise to tumors or are generated within an existing tumor still remains an unanswered question. Some view that tumors originate from mutant forms of progenitor cells, adult stem cells or adult progenitor cells that acquire stem cell properties. Others favor the idea that mutation in the stem cells within their niche during development initiates tumors [17]. According to a different conceptual framework, the tumor is made up of several types of stem cells. Among these, only one remains viable in the specific microenvironment that harbors them while others, under the same conditions, are less successful lines. These other lines, however, can become more successful in adapting to other microenvironments or prevail in response to treatment [18]. Another appealing idea is that acquisition of stem cell like characteristics results from dedifferentiation of cancer cells. Such a notion is supported by a growing number of reports showing that inflammation or damage can cause dedifferentiation and generation of cells that exhibit a stem like phenotype [19–20].

It is well known that tumor cells can recover from various types of damage including X-radiation, oxidative stress, and hypoxia. These early studies suggested that the pH and level of glucose are the primary factors that play a crucial role in recovery of cancer cells from Potentially Lethal Damage (PLD) [21–22]. Reduced thiols and particularly glutathione are involved in cellular repair mechanisms [23] and there is compelling evidence that hydrogen sulfide (H_2S) plays a prominent role in cell survival by regulating intracellular redox homeostasis through cysteine-GSH connection [24]. H_2S is a gasotransmitter and its intracellular production is enzymatically regulated. There are three enzymes, which control the production of H_2S, namely, cystathionine β-synthase (CBS), Cystathionase (CTH) also known as cystathione γ-lyase (CSE) [25–26], and 3-mercaptopyruvate sulfurtransferase (MST) [27–28]. H_2S is produced in many different cell types and due to its lipophilic nature, can easily diffuse without the need for transporters [29]. In normoxic tissues, exogenous H_2S is rapidly metabolized, whereas in anoxic tissues, H_2S is unaffected, protecting cells against hypoxia-induced injury [30–31].

Recently, we reported that cancer cells that recover from a potentially lethal damage display mitochondrial reorganization and increased drug resistance [32] similar to that which is found in induced pluripotent stem cells (iPS). Here, we demonstrate that upon recovery from a potentially lethal damage induced by oxidative stress, hypoxia, or glucose deprivation, cancer cells undergo dedifferentiation characterized by reactivation of expression of a repertoire of stem cell genes and plasticity to transdifferentiate into another cell phenotype. This phenomenon is dependent on the production of H_2S and up-regulation of Nampt. H_2S acts as an inducer of Nampt, whereas Nampt, controls the expression level of H_2S generating enzymes and, thus, it fine tunes the level of intracellular H_2S. We also show that cancer cells that are exposed to exogenous H_2S express stem cell markers in a manner similar to that exhibited by cancer cells that recover from a potentially lethal damage. These data show that cancer cells modify their phenotype and gene expression pattern and dedifferentiate by a molecular switch comprised of H_2S and Nampt.

Materials and methods

Materials

Chemicals were purchased from Sigma-Aldrich Company (St Louis, MO) or Fisher Scientific (Pittsburgh, PA). RNeasy Mini Kit for total RNA isolation was purchased from Sigma-Aldrich. Nampt, SSEA1 and SSEA4 antibodies were from Abcam (Cambridge, MA), CBS and CTH antibodies were from Santa Cruz Biotechnology (Santa Cruz, CA), β-actin antibody was from Millipore (Billerica, MA) and secondary antibodies were purchased from Jackson ImmunoResearch Laboratories (Baltimore, PA). H_2S fluorescent probe HSN2 was a kind gift from Professor Michael D. Pluth, University of Oregon, Department of Chemistry, Eugene, Oregon. *NAMPT*-specific siRNA was purchased from Santa Cruz Biotechnology.

Cell culture

CT26 mouse colon carcinoma cell line (CRL-2639), HepG2, MDA-MB-231 and -435S cell lines were obtained from ATCC (Manassas, VA). CT26 cells were cultured in RPMI 1640 with 2 mM glutamine, 10 mM HEPES, 1 mM sodium pyruvate, 25 mM glucose, 1.5 g/L sodium bicarbonate, whereas HepG2, MDA-MB-231 and -435S were maintained in DMEM with 2 mM glutamine and 25 mM glucose, 0.1 mM non-essential amino acids and 10% fetal bovine serum, in a 37°C incubator with 5% CO_2. Parental control (Pc) and damage recovered (DR) cells were maintained in the same media supplemented with 10% FBS. Pc cells were also maintained in α-MEM medium supplemented with 5% FBS on either adherent or ultra-low attachment suspension culture plates. Spheroid colonies

(Sp) were isolated from damage recovered cells and were maintained on ultra-low attachment suspension culture plates in α-MEM media (Invitrogen, Carlsbad, CA) supplemented with 5% FBS, 4 μg/ml heparin, 20 ng/ml bFGF and 100 ng/ml EGF to facilitate the Sp self-renewal. For expansion, spheroids were dissociated with 0.05% trypsin/EDTA (Invitrogen) and passed every 5 days in low-adherent suspension culture dishes (USA Scientific, Ocala, FL). Only Sp and not parental cells maintained 3D structures and expressed markers of stemness when grown on a low adhesion suspension culture plates in the medium supplemented with 5% FBS (Supplementary Fig. 1A–B). Spheroids could be dissociated by trypsinization and re-plated weekly for three months without evidence of loss of self-renewal ability or loss of viability (Supplementary Fig. 1C).

Animal experiments

Animal care and all procedures carried out following approval of the Institutional Animal Care Committees of University of California, Irvine (protocol number 2012-3042). The study included 10 eight-week-old, male athymic nude (Nu/Nu) mice, (Charles River Laboratories, San Diego CA). Each athymic nude mouse received 10^5 cells in a total volume of 100 μl subcutaneously in four locations in the mid-abdominal and lower flank areas. Half hour before the tumor cell injection, animals were anesthetized by inhalation of 1.5% isoflurane. Animals were monitored for appearance, activity, pain and distress two to three times weekly. Experimental time course varied depending on the type of tumor. Mice were euthanized when the tumors grew to ~1.5 cm in diameter. At the end of the experiments, mice were euthanized and tumors were removed, dissected out and viable and damaged tumor cells were isolated.

Whole cell protein extraction and Western blotting

Proteins from cells were extracted in lysis buffer (50 mM Tris–HCl, pH7.5, 150 mM NaCl, 1% NP-40, 2 mM EDTA, 1 mM PMSF, 1 mM Na_3VO_4, 50 mM NaF, and protease inhibitor cocktail). Protein measurements were carried out by Bio-Rad protein assay based on Bradford dye-binding method (Bio-Rad Lab, Hercules, CA).

Blots were probed with antibodies as detailed in the results. Bands were detected by ECL enhanced chemiluminescence (Amersham ECL Plus Western Blotting Detection Reagents, GE Healthcare Life Sciences, Pittsburgh, PA) using C-Digital Imager (Li-COR, Lincoln, NE). Densitometric analysis was performed using myImage Analysis software (Thermo Scientific, New Hampshire). β-actin served as a loading control.

Reverse transcription-polymerase chain reaction (PCR) and quantitative PCR (qPCR)

Total RNA was isolated using GenElute™ Mammalian Total RNA Miniprep Kit (Sigma-Aldrich). Reverse transcription was performed using High-Capacity cDNA Reverse Transcription Kit (Invitrogen).

Gene expression was assessed by PCR using Taq 5X Master Mix (New England Biolabs. Ipswich, MA) with an initial denaturation step at 94°C for 5 min, followed by 30 cycles with each at 94°C for 30 sec 55°C for 30 sec, and 68°C for 1 min. Quantitative evaluation was performed by using myImage Analysis software (Thermo Scientific). For normalization of data, gene expression was assessed by qPCR using SYBR Green PCR Kit (Biorad). The plate was read at every cycle at the predetermined temperature based on the product melting curve. Sequences of the used primers for the analyzed genes are shown in Table 1.

Table 1 – Sequence of RT-PCR and real time primers.

Gene description[1]	Product size (bp)	Forward primer	Reverse primer
β–ACTIN	221	AAGCCACCCCACTTCTCTCT	GAGACCAAAAGCCTTCATACATCT
NANOG	237	TTGGGACTGGTGGAAGAATC	GATTTGTGGGCCTGAAGAAA
KLF4	396	*ACGATCGTGGCCCCGGAAAAGGACC*	*TGATTGTAGTGCTTTCTGGCTGGGCTCC*
OCT4	335	AGGTGTTCAGCCAAACGACC	TGATCGTTTGCCCTTCTGGC
OCT4A	380	*CTCCTGGAGGGCCAGGAATC*	*CCACATCGGCCTGTGTATAT*
OCT4B	302	*ATGCATGAGTCAGTGAACAG*	*CCACATCGGCCTGTGTATAT*
SSEA1	191	*CTTCAACTGGACGCTCTCCTA*	*GTTGGTGGTAGTAGCGGACC*
DPPA2	188	*GGTGCCAGTTAAAGATGACGC*	*GAGGCAAAATGGTCGGCAAG*
FBXO15	216	*CCCACCAAACATAGACTCCGA*	*CGAGCCTAATGTGCTCCTCT*
SOX2	150	*GGGAAATGGGAGGGGTGCAAAAGAGG*	*TTGCGTGAGTGTGGATGGGATTGGTG*
α–FETOPROTEN (AFP)	280	*GAATGCTGCAAACTGACCACGCTGGAAC*	*TGGCATTCAAGAGGGTTTTCAGTCTGGA*
E-CADHERIN	200	TGCCCAGAAAATGAAAAAGG	GTGTATGTGGCAATGCGTTC
SNAIL	134	CATCTGAGTGGGTCTGGAGG	CTTCTCTAGGCCCTGGCTG
CBS	286	*GAACCAGACGGAGCAGACAA*	*GTCGCTCAGGAACTTGGTCA*
CTH	204	*AAAGACGCCTCCTCACAAGG*	*AAGGCAATTCCTAGTGGGATTTC*
MTS	239	*CGCCGTGTCACTGCTTGAT*	*CAGGTTCAATGCCGTCTCG*
CYTOKERATIN 18	216	*GGCATCCAGAACGAGAAGGAG*	*ATTGTCCACAGTATTTGCGAAGA*
ADIPONECTIN	248	*TGCTGGGAGCTGTTCTACTG*	*TACTCCGGTTTCACCGATGTC*
NAMPT	172	*ATCCTGTTCCAGGCTATTCTGT*	*CCCCATATTTTCTCACACGCAT*
MYOGENIN	341	*GGGGAAAACTACCTGCCTGTC*	*AGGCGCTCGATGTACTGGAT*
FIBRONECTIN	200	*GAGAATAAGCTGTACCATCGCAA*	*CGACCACATAGGAAGTCCCAG*

[1] ***Homo sapiens***, PCR: polymerase chain reaction, bp: base pair, [1]Numbers show start sites of the primers.

Knockdown of *NAMPT* by small interfering RNAs

Pools of three to five 19–25 nt *NAMPT*-specific siRNAs were designed to knockdown *NAMPT* gene expression. For successful gene transfection, spheroid colonies were dissociated by trypsinization into a single cell suspension (2×10^5 cells). Cells were incubated in 6 cm dishes in 5% serum MEM medium supplemented with Lipofectamin containing 50 pmol of either *NAMPT*-specific siRNA or control siRNA with a scrambled sequence. Cells were transfected for 3 days. To determine the efficacy of transfection, the expression of *NAMPT* was analyzed by RT-PCR and qPCR.

Histochemical staining

Fluorescence imaging of H_2S in live cells was obtained with H_2S fluorescent probe HSN2 (a kind gift of Professor Michael D. Pluth, University of Oregon, Department of Chemistry, Eugene, Oregon) by incubating cells in 5 μM HSN2 for 30 min.

For alkaline phosphatase staining, cells were fixed and stained with NBT/BCIP solution in NTMT (100 mM Tris pH 9.5, 100 mM NaCl, 0,1% Tween-20) for 2 h at room temperature. Color reaction was stopped by washing cells in phosphate buffered solution, and samples were examined microscopically. Positive staining was indicated by distinct brown staining.

For SSEA1 and SSEA4 immunostaining, cell cultures were fixed for 5 min in 2% buffered paraformaldehyde containing 0.02% NP40. Cells were subjected to blocking for 10 min in 2% serum. Cells were then incubated with the primary antibodies (1–2 μg/ml) followed by the secondary antibody (1–2 μg/ml). The staining was developed in 3,3'-diaminobenzidine (DAB)–H_2O_2 and viewed at the light microscopic level without counterstain.

Cell viability measurement

Relative cell number was measured by XTT assay (Sigma-Aldrich). Cells were incubated with XTT and phenazine methosulfate (PMS) at 37 °C for 2 h and absorbance was read at 450 nm and 650 nm as reference.

Quantitation of Nampt, NAD^+/NADH and thiols

Intracellular Nampt levels were measured using a Visfatin C-terminal (Human) EIA kit (Phoenix pharmaceuticals, Belmont, CA, USA).

NAD^+/NADH levels were measured using NAD^+/NADH assay kit (Cayman Chemical Company, Ann Arbor, MO and BioAssay Systems, Hayward CA) according to manufacturer's instruction.

Total thiols were quantitated by reaction of cells with 5,5'-Dithio-bis(2-nitrobenzoic acid) (DTNB) and measurement of absorbance at 412 nm. Thiols content was estimated from a cysteine standard curve obtained in parallel for each assay.

Levels of NAD^+, NADH and thiols were normalized to the protein content.

Measurement of H_2S production

Measurement of extracellular H_2S level was performed using Free Radical Analyzer (TBR4100 and ISO-H2S-2, World Precision Instruments, Sarasota, FL) in accord with the manufacturers' instruction. Briefly, sample cells were adjusted to 1×10^6 viable cells per test with PBS, and the cell suspensions were incubated in 37°C incubator for 1 h. Cells were then centrifuged and the supernatants were subjected to measurements. Prior to the measurement, the sensor was polarized and calibrated by adding four aliquots of the Na_2S stock solution at the final concentrations of 0.25, 0.5, 1.0 and 2.0 μM.

Statistics

All assays were done in 3–6 replicates in at least three independent experiments. Data are shown as mean ± SEM. *P* values were determined by comparing the data from experimental versus control cells from at least three independent experiments or six replicates of the same experiment. Means and *p* Values for experimental data were analyzed by subjecting the data to the two tailed *t*-test. *p* values less than 0.05 were considered significant. *P* values are shown as <0.05 (*), <0.005 (**) or <0.0005 (***).

Results

Spheroids are formed by cancer cells that recover from a potentially lethal damage

We chose hydrogen peroxide to induce injury in cancer cells since it is produced in relatively large amounts by some tumor cells reaching rates up to 0.5 nmol/10^4 cells/h [33]. Exposure of HepG2 cells to hydrogen peroxide resulted in cell death with LD_{50} being 800 μM. The pretreatment of cells with NaHS, a donor of H_2S, for 18 h significantly attenuated the effect of hydrogen peroxide (Fig. 1A). Similar effect of NaHS was observed in MDA-MB-231 cells exposed to H_2O_2 for 3 h (Supplementary Fig. 2A). Consistent with previous reports, protective effect of NaHS was due to modulation of thiol homeostasis leading to increased total level of reduced thiols (Fig. 1B). Within 24 h after treatment with H_2O_2, few viable (trypan blue negative) cells remained attached to the culture flask while majority of cells detached due to mitosis or severe damage (Supplementary Fig. 2B–C). To isolate potentially lethal damage-recovered (DR) cells, we first removed the mitotic and all viable cells by culturing cells in new culture vessels for 24 h. Then, floating cells that failed to bind to culture vessels but had the potential to recover from damage were transferred to new culture vessels. Serial weekly passages of floating cells to new culture vessels for duration of 2 weeks allowed isolation of damage-recovered (DR) cells. In cells which recovered from damage induced by hydrogen peroxide (DR^{H2O2}) and began to proliferate, the γ-H_2AX level was low (Fig. 1C). The dephosphorylation of H_2AX in DR cells signaled the completion of repair [34]. The level of reduced thiols increased in DR cells compared with parental control cells (Pc) (Fig. 1D, Supplementary Fig. 2D) indicating that endogenous H_2S might play a cytoprotective role in potentially lethal damage recovery (PLDR). Indeed, increase in the level of thiols was associated with increase in H_2S in cells that recovered from damage (Fig. 1E–F). We have employed two techniques to study intracellular production of H_2S. The H_2S release was measured by using sulfide-sensitive electrode and intracellular H_2S synthesis was visualized by the fluorescent probe, Hydrosulfide Naphthalimide-2 (HSN2), a kind gift of

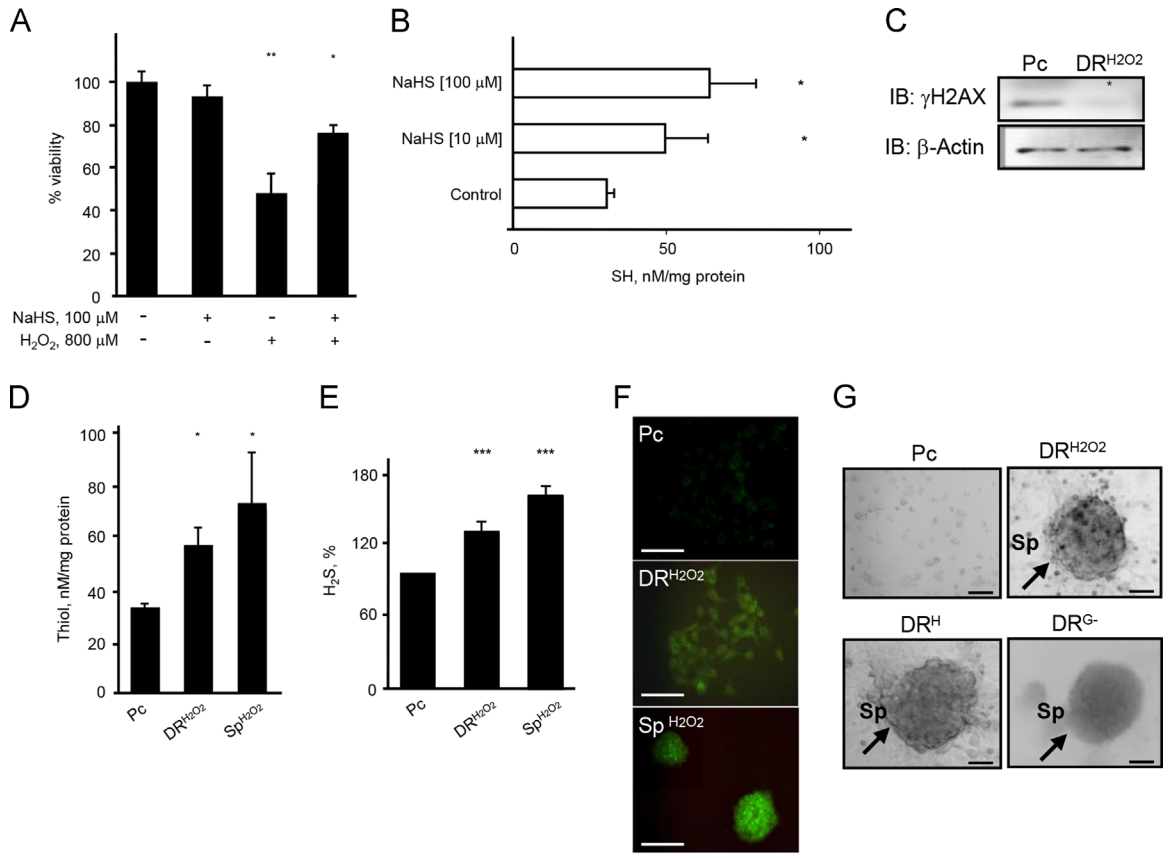

Fig. 1 – Endogenous hydrogen sulfide level increases in cancer cells after recovery from a potentially lethal damage. A. Cell viability was measured by XTT assay in HepG2 cells pre-treated for 24 h with 100 μM of NaHS and then subjected to H_2O_2 (800 μM) for 3 h. B. Total level of thiols in Pc HepG2 cells treated for 24 h with 0, 10, and 100 μM of NaHS. The levels of thiol were normalized to the level of total protein. C. The level of γH2AX assessed by western blot analysis in HepG2 Pc and DR^{H2O2} cells. D. Total thiol levels in HepG2 Pc, DR^{H2O2} and Sp^{H2O2} cells. The levels of thiol were normalized to the level of total protein. E. Amount of H_2S released by HepG2 Pc, DR^{H2O2} and Sp^{H2O2} cells. F. H_2S staining of HepG2 Pc, DR^{H2O2} and Sp^{H2O2} cells stained with 5 μM H_2S fluorescent probe, HSN2. Scale bars, 100 μM. G. Representative images of emerging spheroid-forming cells in HepG2 cells recovered from damage induced by hypoxia (Sp^{H}), glucose deprivation (Sp^{G-}) and treatment with hydrogen peroxide (Sp^{H2O2}). Arrows point to the emerging spheroids. Scale bars, 50 μM. *; $p<0.05$, **; $p<0.005$, *; $p<0.0005$.**

Professor Michael D. Pluth. HSN2 provides a robust intensity and high selectivity for H_2S over oxygen and nitrogen and other reactive sulfur species such as cysteine and glutathione [35]. Using this probe, the parental control cells are dim while the DR cells exhibit an intense fluorescence (Fig. 1F).

We also observed that a population of DR^{H2O2} cells forms 3D spheroid (Sp^{H2O2}) structures which are surrounded by a monolayer of cells. In contradistinction, the parental cells fail to form similar structures under identical culture conditions in standard culture media supplemented with 10% FBS (Fig. 1G). Similar DR cells forming spheroids appeared following recovery from damage induced by hypoxia (O_2 level below 1%) for 18 h (Sp^{H}) or glucose deprivation for 18 h (Sp^{G}). The compact multi-cellular spheroid colonies were consistently formed independent of the type of damage that cells endured or the type of cells that were damaged (HepG2, MDA-MB-231, MDA-MB-435S, and CT26) (Fig. 1G, Supplementary Fig. 2E). The highest increase in H_2S production was observed in 3D spheroids as compared to other cancer cells in the same dish that grew as a monolayer and failed to form spheroids (Fig. 1E–F). The increased cell–cell interaction in 3D cultures was associated with modification of gene expression and alteration of cell–cell adhesion as evidenced by expression of E-cadherin. To study these spheroids in more details, spheroids were cultured in a medium which was supplemented with 5% FBS on low adhesion plates to promote self-renewal.

Spheroids formed following recovery from potentially lethal damage show enhanced H_2S-producing activity

The relative level of mRNA for *CBS* and *CTH* increased in DR^{H2O2} cells with highest increase in Sp^{H2O2} colonies (Fig. 2A–B). There was also a significant difference in the level of *MST* mRNA in Pc, DR^{H2O2} and Sp^{H2O2} cell populations (Fig. 2A). The *MST* mRNA was undetectable in both Pc and DR^{H2O2} cells whereas its expression was readily detected in DR derived Sp^{H2O2} cells. The endogenous CTH and CBS protein levels increased over 2 folds in spheroid colonies (Fig. 2C–D). It is known that infusion of H_2S may change the NAD^+ level [36]. We found that after recovery from damage, NAD^+ was significantly increased in cancer cells forming Sp colonies (Fig. 2E).

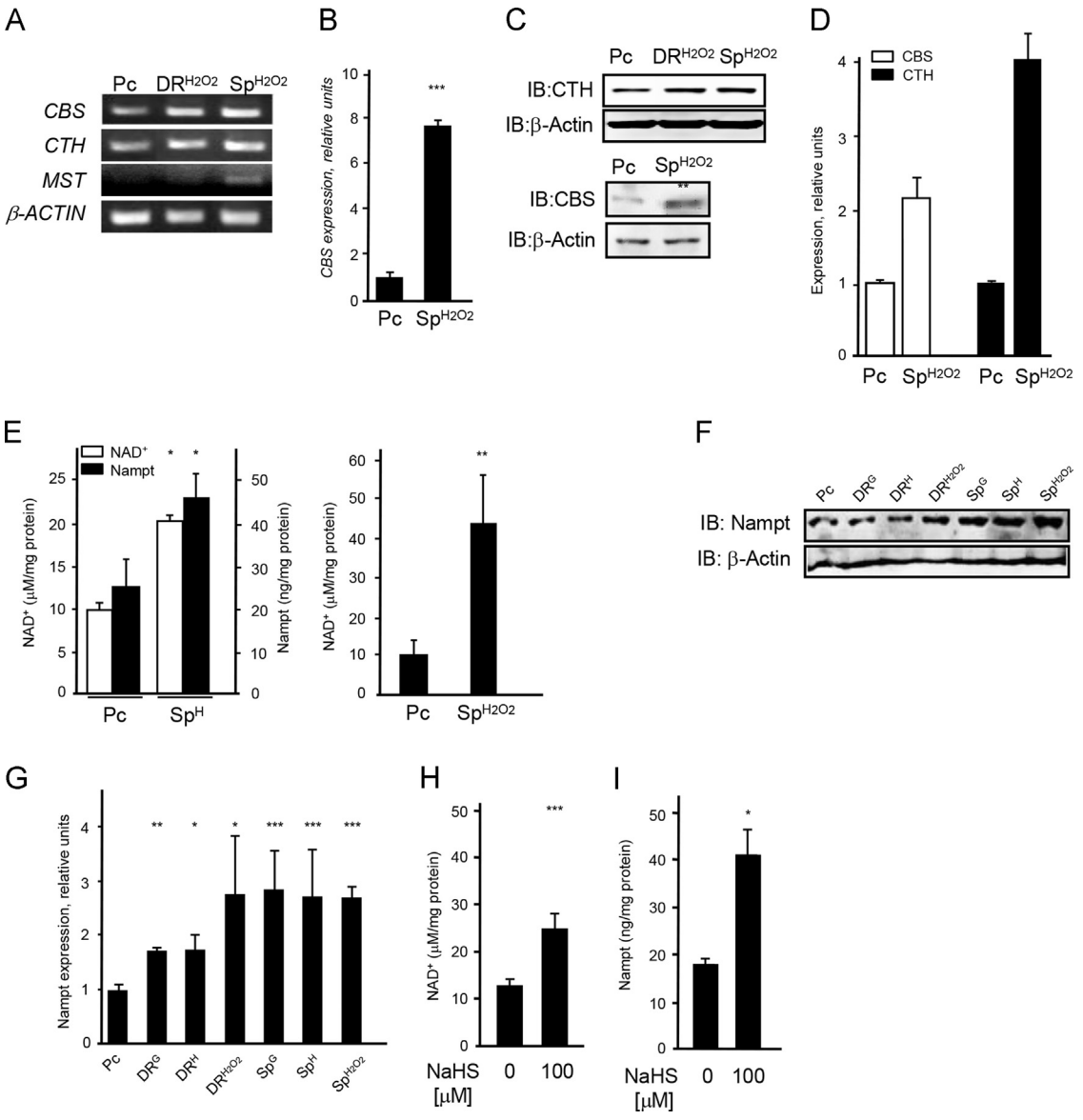

Fig. 2 – Recovery from potentially lethal damage requires activation of Nampt. A. *CBS*, *CTH* and *MST* gene expression levels were evaluated by RT-PCR analysis in DR^{H2O2} and DR derived spheroid cells (Sp^{H2O2}) generated under oxidative stress induced by H_2O_2. B. *CBS* mRNA expression in Sp^{H2O2} cells relative to Pc cells. The expression level was measured by real time PCR analysis and normalized with the expression of β-actin. C. Western blot analysis of CTH and CBS protein expression in DR^{H2O2} cells and DR derived Sp^{H2O2} cells. β-actin *was used as a loading control.* D. Relative level of CTH and CBS proteins normalized to β-actin. E. Left panel: The contents of NAD$^+$ and Nampt were measured in HepG2 Pc and Sp^H cells. Right panel: The content of NAD$^+$ was measured in HepG2 Pc and Sp^{H2O2} cells. NAD$^+$ and Nampt levels were normalized to the level of total protein. F. Western blot analysis of Nampt in DR cells and spheroids (Sp) generated under glucose deprivation (^{G}), hypoxia (^{H}) and oxidative stress induced by H_2O_2 (^{H2O2}). G. Relative level of Nampt protein normalized to β-actin. Levels of NAD$^+$(H) and Nampt (I) in HepG2 Pc cells treated with 100 μM of NaHS for 48 h. Nampt protein level was determined by ELISA based assay. *; $p<0.05$,; $p<0.005$, ***; $p<0.0005$.**

The up-regulation of H_2S generating enzymes, *CBS* and *CTH* coincided with increase in Nampt, which is required for synthesis of NAD$^+$ and repair (Fig. 2F–G). The observed increase in Nampt was independent of type of damage. To further assess the importance of H_2S in upregulation of Nampt, Pc cells were treated with H_2S donor, NaHS. Similar to our observations in DR^{H2O2} and Sp^{H2O2} cells, treatment of Pc cells with NaHS increased level of Nampt and coordinately increased NAD$^+$ output (Fig. 2H–I). Accumulation of H_2S and increased synthesis of NAD$^+$ resulted in increased tolerance of DR cells towards damage and nutrient depletion. Compared to Pc cells, cells recovered from damage showed increased resistance to such cancer drugs as cisplatin or bleomycin (Supplementary Fig. 3A–C) to nutrient deprivation (Supplementary Fig. 3D).

Endogenous hydrogen sulfide generated by cancer cells recovered from damage directs cells into acquisition of a dedifferentiated state

The observed altered cancer cell phenotype as manifested by the formation of 3D spheroids suggested that these DR cells undergo

dedifferentiation. To determine whether cells forming spheroidal colonies contain undifferentiated cells, we studied the expression of several genes characteristic of stem cells. To examine expression profile of *OCT4*, we designed primers that avoided amplification of *OCT4* pseudogenes. Furthermore, we used primers that distinguish between *OCT4A* isoform, which is highly expressed in ESC, and *OCT4B* variant, which is up-regulated only in response to damage [37–38]. Compared to the Pc cells, the DR derived Sp cells had an elevated level of expression of *OCT4A*, *NANOG*, *KLF4* (*Kruppel-Like Factor 4*), *SSEA1* (*Stage-Specific Embryonic Antigen*), *DPPA2* (Developmental Pluripotency Associated 2 gene), and *FBXO15*, while expression of damage inducible *OCT4B* was negligible (Fig. 3A, Supplementary Fig. 4A–D). Only DR and Sp cells expressed stem cell markers such as *OCT4* and *NANOG* (Fig. 3B and Supplementary Fig. 4C–D). The level of expression of *OCT4* and Oct4 protein were also up-regulated in DR cells as compared to that detectable in Pc cells (Fig. 3B–C). Increase in *OCT4* expression associated with staining for Oct4 protein (shown in red) in CT26 DR^H cells clearly indicates that the expression of *OCT4* is not due to expression of stress induced *OCT4B* variant or *OCT4* pseudogenes (Fig. 3C). CT26 DR^H cells were positively stained for glycolipid antigens SSEA1 and SSEA4, surface markers for undifferentiated stem cells (Fig. 3D). The dedifferentiation of Sp cells was further confirmed by alkaline phosphatase staining, which is a sensitive indicator of an undifferentiated state (Fig. 3E) [39]. The expression of stem cell markers was associated with accumulation of H_2S and increased NAD^+ and Nampt. In order to validate the functional role of H_2S in dedifferentiation, we explored the efficiency of NaHS in inducing expression of stem cell markers. The treatment of Pc cells with NaHS led to expression of *OCT4* and *NANOG*, while *HIF1α* expression was down-regulated (Fig. 3F). NaHS also increased the level of *E-CADHERIN* (Fig. 3F), which was shown to be essential for the maintenance of cell integrity and an undifferentiated state [40].

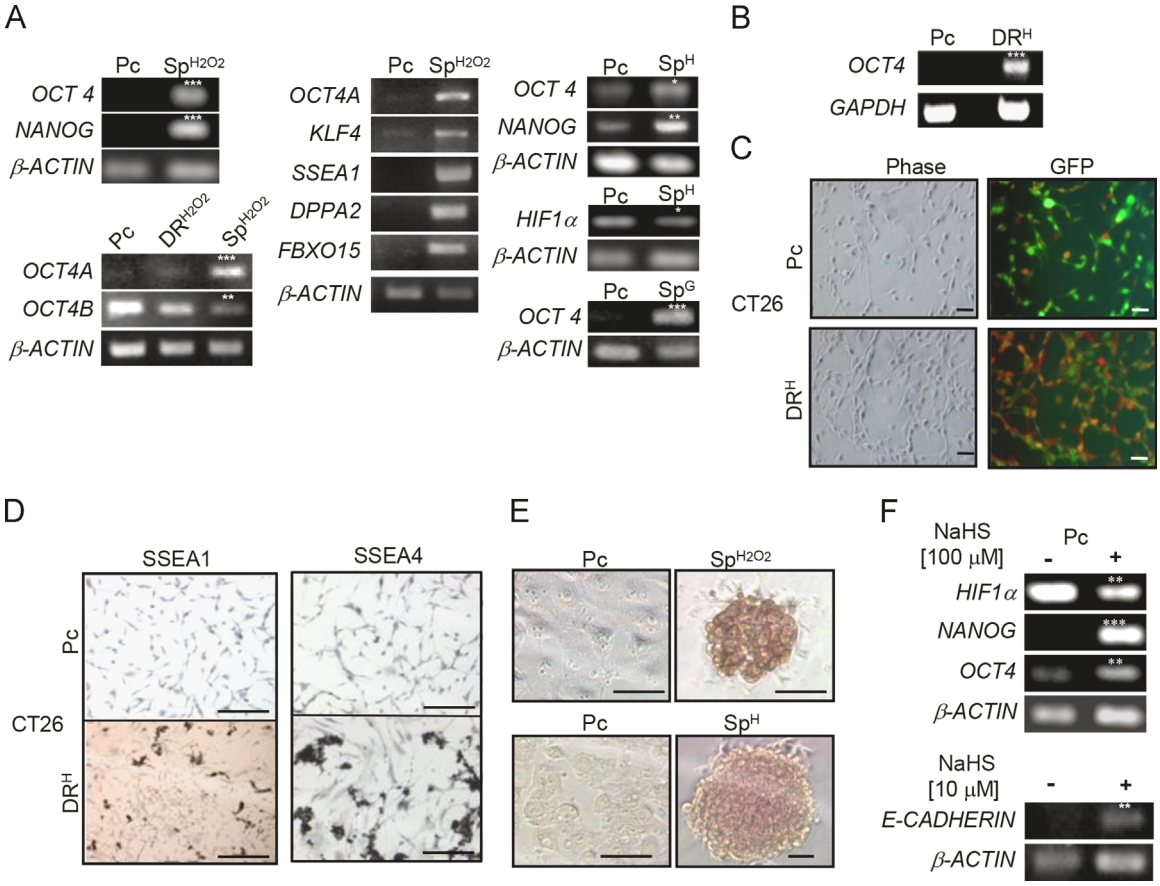

Fig. 3 – Damage Recovered (DR) cells forming 3D spheroids exhibit an undifferentiated phenotype. A. *OCT4* (*A/B*), *NANOG*, *KLF4*, *SSEA1*, *DPPA2*, *FBXO15* and *HIF1α* gene expression levels in HepG2 Pc, Sp^{H2O2}, Sp^H and Sp^G cells were assessed by RT-PCR analysis. *β-ACTIN* gene expression level served as a loading control. B. RT-PCR analysis of *OCT4* gene expression in CT26 Pc and DR^H cells. GAPDH gene expression level served as a loading control. C. Oct4 protein expression in CT26 DR^H cells. Monolayer culture of CT26 parental Pc and DR^H GFP labeled CT26 cells viewed under phase contrast (left panel) and GFP and Oct4 protein labeled under fluorescent microscope (right panel). Red staining indicates Oct4 protein. Immunofluorescence staining revealed that a majority of DR^H cells were Oct4-positive. Scale bars, 100 μM. D. Immunostaining of SSEA1 and SSEA4 in CT26 parental Pc and DR^H cells. E. Alkaline phosphatase staining of HepG2 Pc, Sp^{H2O2} and Sp^H cells. Scale bars, 100 μM. F. RT-PCR analysis of *HIF1α*, *NANOG*, *OCT4*, and *β-ACTIN* in Pc HepG2 cells treated with 0 and 100 μM of NaHS for 48 h and *E-CADHERIN* in HepG2 Pc cells treated with 0 and 10 μM NaHS for 24 h. *; $p<0.05$,; $p<0.005$, ***; $p<0.0005$.**

H_2S induces dedifferentiation in a Nampt-dependent manner

As expected, the treatment of DR cells with DL-propargylglycine (PAG) that inhibits CBS and CTH reduced H_2S accumulation (Fig. 4A). Most strikingly, although, there was no cytotoxicity in cancer cells treated with FK866 observed after 24 h (data not shown), treatment of HepG2 cells with FK866 inhibited Nampt, and decreased the production of H_2S (Fig. 4A). Consistent with change in H_2S production, the levels of CBS and CTH protein expression were diminished by treatment with FK866 (Fig. 4B). The treatment of HepG2 Sp^{H2O2} cells with FK866 led to down-regulation of *CBS* gene expression and coordinately caused a 2 fold decrease in H_2S production (Fig. 4C–D). Inhibition of H_2S by PAG abated the expression of *OCT4*, *NANOG* and *E-CADHERIN* in Sp cells, showing that expression of stem cell markers in Sp cells is H_2S driven (Fig. 4E–G). Similar levels of suppression of stem cell markers was achieved by treatment of Sp cells with FK866 (Fig. 4E–F). Suppression of *NAMPT* by FK866 decreased expression of stem markers, *KLF4*, *NANOG*, *SOX2*, and *FBOX15* (Fig. 5 A–B). To further validate the role of Nampt on dedifferentiation, we carried out a *NAMPT* knockdown experiment using *NAMPT* siRNA. Spheroid HepG2 colonies were dissociated by trypsinization into a single cell suspension for successful transfection. *NAMPT* expression was diminished only in cells that were transfected with the siRNA to *NAMPT* and not by non-target specific scrambeled siRNA (Fig. 5A and B). However, no change in the expression of *OCT4A/B*, *DPPA2* and *SSEA1* was found in cells that were transfected with *NAMPT* siRNA. *NAMPT*-knockdown by Nampt siRNA diminished the expression of *CBS* leading to reduced intracellular production of H_2S (Fig. 5A and C). However, expression of *CTH* was not affected by Nampt siRNA (Fig. 5C). Furthermore, we observed that *NAMPT*-knockdown prevented the formation of spheroidal colonies. Interestingly, *NAMPT* depleted cells exhibited single cells and led visibly to formation of small 'stressed' spheres, whereas in cells that were treated with control siRNA, spheroids were formed 3 days after transfection (Fig. 5D).

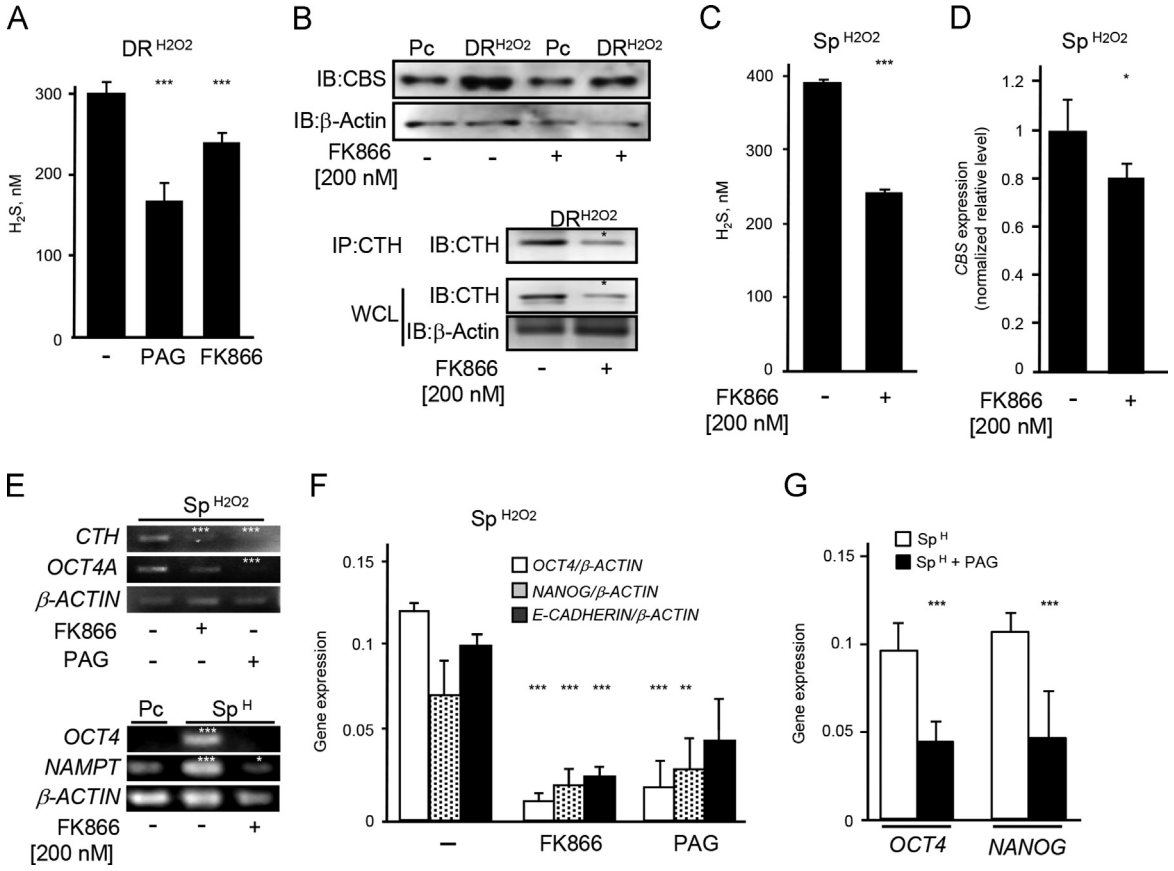

Fig. 4 – H_2S and Nampt promote an undifferentiated phenotype. A. Amount of H_2S released from DR^{H2O2} HepG2 cells treated with CTH inhibitor, PAG (100 μM, 18 h), and Nampt inhibitor, FK866 (200 nM, 24 h). B. Immunoblotting (IB) analysis of CTH and CBS in DR^{H2O2} HepG2 whole cell lysate (WCL) in the absence and presence of FK866 (200 nM, 24 h). Immunoprecipitation (IP) of CTH from DR^{H2O2} cells treated with FK866 and immunoblotting (IB) analysis of the immunoprecipitates with anti-CTH antibody. C. Amount of H_2S released from Sp^{H2O2} HepG2 cells treated with Nampt inhibitor, FK866 (200 nM, 24 h). D. Expression level of *CBS* assessed by real time PCR in Sp^{H2O2} HepG2 cells treated with Nampt inhibitor, FK866 (200 nM, 24 h). E. RT-PCR analysis of *OCT4*, *CTH* and *NAMPT* gene expression in Sp^{H2O2} and Sp^{H} HepG2 cells treated with either PAG (100 μM, 18hr) or FK866 (200 nM, 24 h). Real time PCR analysis shows changes in the expression of *OCT4*, *NANOG* and *E-CADHERIN* in Sp^{H2O2} (F) and Sp^{H} (G) cells treated with PAG (100 μM, 18 h), and Nampt inhibitor, FK866 (200 nM, 24 h). Expression levels were normalized with the expression of *β-ACTIN*. *; $p<0.05$,; $p<0.005$, ***; $p<0.0005$.**

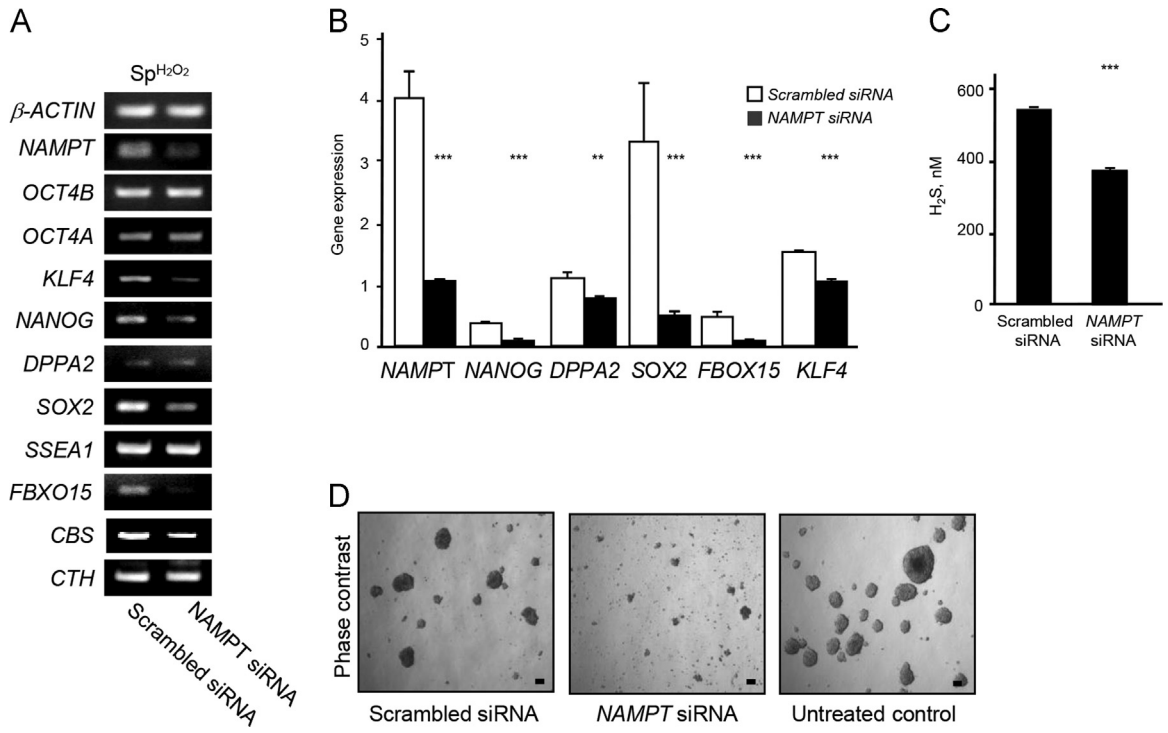

Fig. 5 – Depletion of Nampt by small interfering RNA (siRNA) reduces dedifferentiation capacity of cells recovered from damage. Cells were transfected with *NAMPT* siRNA or scrambled control siRNA. Gene expression (A and B), H_2S production (C) and Sp colony formation (D) were analyzed 72 h later. A. *OCT4* (*A/B*), *NANOG*, *KLF4*, *SSEA1*, *DPPA2*, *FBXO15*, *CBS* and *CTH* gene expression levels in HepG2 Sp^{H2O2} cells were assessed by RT-PCR analysis. *β-ACTIN* gene expression level served as a loading control. B. Real time PCR analysis shows changes in the gene expression in Sp^{H2O2} cells transfected with *NAMPT* siRNA. C. Amount of H_2S released by Sp^{H2O2} cells transfected with *NAMPT* siRNA or scrambled control siRNA. D. Representative phase contrast images of spheroids formed from single Sp^{H2O2} cells transfection with *NAMPT* siRNA or scrambled control siRNA.

Accumulation of H_2S leads to the dedifferentiation of cancer cells in *in vivo* generated tumors

To identify whether cells similar to *in vitro* generated Sp cells exist or can be generated in tumors, epithelial cancer cells of different lineages were inoculated into immunodeficient mice. Tumors that grew subcutaneously were removed, and were subjected to collagenase treatment.

The isolation of viable tumor (T^V) cells and damaged (T^{DR}) tumor cells was followed as described in our previous study [32]. Within 1 week, similar to *in vitro* generated DR cells, T^{DR} cells formed 3D spheroid (T^{Sp}) structures along with a monolayer of cells (Fig. 6A, Supplementary Fig. 5A). T^{Sp} colonies, generated in the midst of T^{DR} cells, were comprised of cells that formed cohesive colonies with distinct colony borders. As compared with viable cells isolated from tumors (T^V), T^{Sp} cells produced the highest amounts of H_2S (Fig. 6B–C, Supplementary Fig. 5B–C).

Given the importance of redox homeostasis in the regulation of stem cells, we found that T^{Sp} cells showed diminished NAD^+/NADH ratio and a greatly elevated intracellular thiol levels consistent with accumulation of H_2S and a more reduced redox state (Fig. 6D–E). Importantly, although NAD^+/NADH ratio decreased, the total levels of NAD^+ and NADH were increased (Fig. 6E). *NAMPT* gene and protein expression were also significantly increased in T^{Sp} cells (Fig. 6F–G).

The T^{Sp} cells expressed stem cell markers including *OCT4*, *NANOG*, *E-CADHERIN*, *SOX2* and *AFP* (Fig. 7A–B, Supplementary Fig. 6A–B). These cells were alkaline phosphatase positive, a phenotypic marker of stem cells (Fig. 7C). The T^{Sp} cells expressed *E-CADHERIN*, while the level of *SNAIL*, which induces a switch from *E-CADHERIN* to *N-CADHERIN* was diminished (Fig. 7B, Supplementary Fig. 6B). Treatment of T^{Sp} cells isolated from HepG2 tumors formed in nude mice led to a significantly diminished expression of *E-CADHERIN* (Fig. 7D).

Adipogenic potential of Sp colonies formed by cancer cells recovering from damage

We questioned whether cancer cells which acquire a dedifferentiated phenotype could be forced to differentiate again. The spheroidal DR (Sp^{H2O2}) cancer cells, which expressed the stem cell markers, showed a high degree of plasticity and could differentiate along the adipogenic pathway (Fig. 8A–C). Expression of the adipocyte marker, *ADIPONECTIN*, was higher in Sp^{H2O2} cells rather than Pc cells that were treated with 1% DMSO and this expression coincided with the disappearance of *OCT4A* (Fig. 8A–B, Supplementary Fig. 7A). There was no *ADIPONECTIN* mRNA expression in either Pc or DR cells, which did not show the potential to transition into an undifferentiated state. Despite the expression of *ADIPONECTIN*, Sp^{H2O2} cells also retained cytokeratin 18, a phenotypic marker of epithelial cells (Fig. 8A). To confirm adipogenic differentiation, cells were stained with triglyceride dye, Oil-Red-O. Bright field microscopy of Sp cells growing on gelatin and treated with DMSO revealed these cells to be filled with lipid droplets that

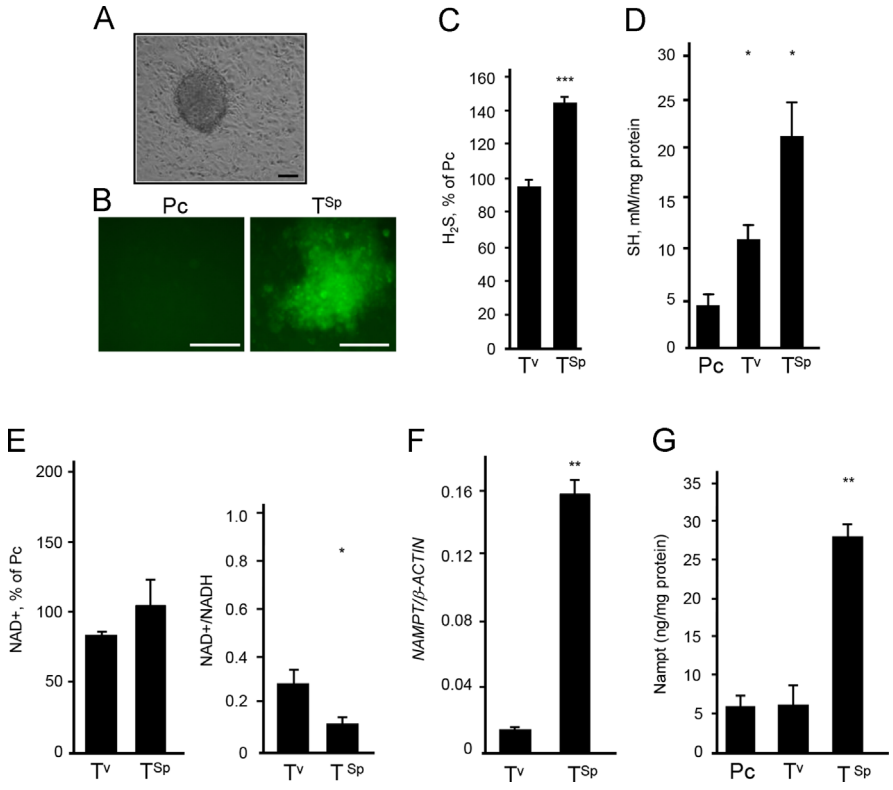

Fig. 6 – Spheroid formation in cells isolated from HepG2 xenograft tumor coincides with elevated levels of H_2S and Nampt. A. Representative phase contrast images of emerging spheroids from cells isolated from *in vivo* generated HepG2 tumors. Scale bars, 100 μM. B. HepG2 (lower panel) Pc and T^{Sp} cells staining with H_2S fluorescent probe, HSN2. Scale bars, 50 μM. C. H_2S in T^v and T^{Sp} cells isolated from *in vivo* generated HepG2 tumors. D. Total thiol levels in T^v and T^{Sp} cells isolated from *in vivo* generated HepG2 tumors. The levels were normalized to the level of total protein. E. Levels of NAD^+ and NAD^+/NADH ratio in T^V and T^{Sp} cells isolated from *in vivo* generated HepG2 tumors. The levels of NAD^+ and NADH were normalized to the level of total protein. F. Expression level of *NAMPT* mRNA assessed by real time PCR in T^V, and T^{Sp} cells isolated from *in vivo* generated HepG2 tumors. G. Nampt protein level assessed by ELISA in T^V, T^{DR} and T^{Sp} cells isolated from *in vivo* generated HepG2 tumors compared with that in Pc HepG2 cells. *; $p<0.05$,; $p<0.005$, ***; $p<0.0005$.**

stained positive with Oil Red O (Fig. 8C). Pc cells treated without or with DMSO failed to show any Oil-Red-O positive cells. The differentiation of Sp^{H2O2} cells along the adipogenic pathway was associated with a decrease in H_2S production and expression of *NAMPT* (Fig. 8D–E). Under the same differentiation condition, in contrast to Sp^{H2O2} cells, Sp^H cells did not exhibit adipogenic differentiation as evident by the lack of positive Oil-Red-O staining and the absence of *ADIPONECTIN* gene expression (data not shown). However under the same conditions, Sp^H cells strongly expressed *MYOGENIN* mRNA while they lost the expression of *OCT4A* (Supplementary Fig. 7A–B). Similar to Sp^{H2O2} cells, upon this differentiation, expression of *NAMPT* was severely diminished in Sp^H cells (Supplementary Fig. 7A). Overall, it is plausible to suggest that diminished H_2S production and downregulation of Nampt result in a more oxidizing cellular environment which is a pre-requisite for differentiation. However, tissue-specific differentiation programs are not predetermined by these changes. T^{Sp} cells isolated from MDA-MB-231 xenograft tumors did not show adipogenic potential (Supplementary Fig. 7C–D). However, similar to HepG2 Sp^{H2O2} cells, T^{Sp} cells isolated from HepG2 xenograft tumors could be forced to differentiate along the adipogenic line as evidenced by ~30 fold increase in *ADIPONECTIN* gene expression in DMSO treated T^{Sp} cells grown on gelatin (Fig. 8F). The increase in *ADIPONECTIN* gene expression was associated with a significant increase in the number and intensity of Oil-Red-O staining in DMSO treated T^{Sp} cells grown on gelatin (Fig. 8G). In contrast to these cells, T^v cancer cells that did not show the ability to form spheroids nor expressed stem cell markers failed to show adipogenic potential when treated with DMSO (Fig. 8G). Instead, these T^{Sp} cells expressed high levels of *FIBRONECTIN*, which is considered a marker of mesenchymal differentiation and a hallmark of epithelial to mesenchymal transition (Supplementary Fig. 7D). Similar to MDA-MB-231T^{Sp}, MDA-MB-435 T^{Sp} cells did not exhibit adipogenic potential (Supplementary Fig. 7C).

Together, our findings show the potential of cancer cells to recover from damage and that such recovery leads to generation of undifferentiated cells with the capability of transdifferentiation.

Discussion

The plasticity of cancer cells and their differentiation has been attributed to changes in the tumor microenvironment [14–16]. Among the putative factors in the microenvironment that modulate plasticity are inter-cellular networks, changes in extracellular matrix, fluctuation in oxygen tension, chronic inflammation triggered by an

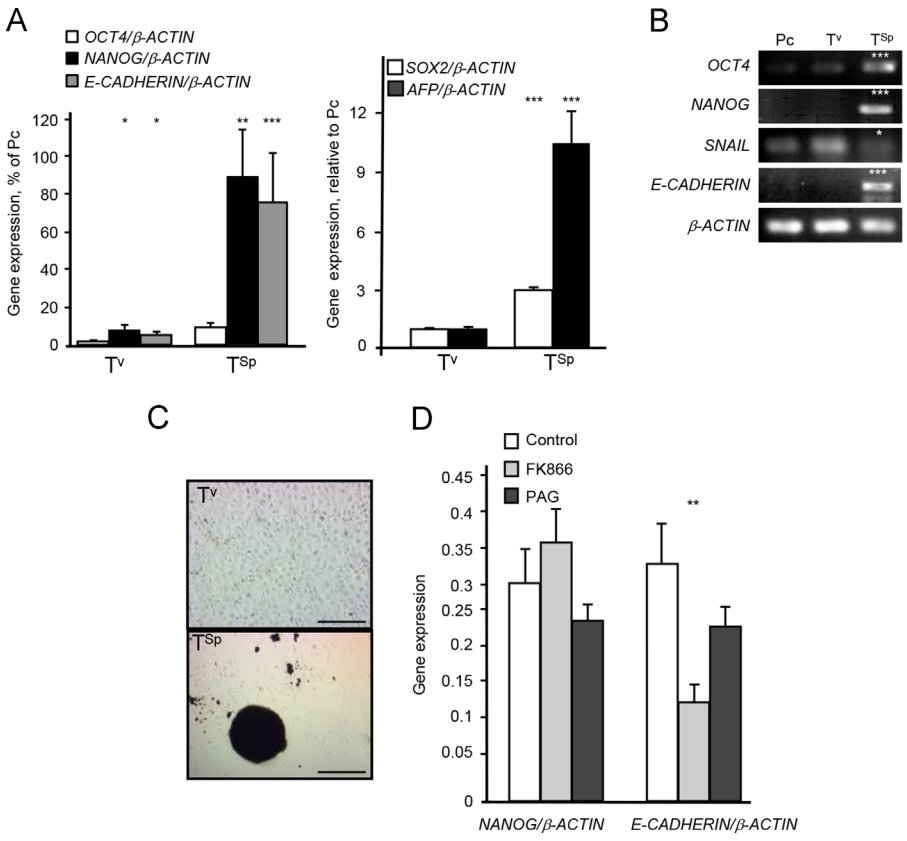

Fig. 7 – Spheroid cells isolated from *in vivo* HepG2 xenograft tumor (T^{Sp}) show expression of stem cell associated genes. A. Expression level of *OCT4*, *NANOG*, *E-CADHERIN*, *SOX2*, and *α-FETOPROTEIN* (*AFP*) assessed by real time PCR. *β-ACTIN* expression was used for normalization. B. RT-PCR analysis of *OCT4*, *NANOG*, *SOX2*, *E-CADHERIN*, *SNAIL* and *β-ACTIN*. C. Representative images of alkaline phosphatase staining in T^{v} cells (upper image) and T^{Sp} cells. Scale bars, 250 μM. D. Expression level of *NANOG* and *E-CADHERIN* assessed by real time PCR in T^{Sp} cells treated with PAG (100 μM, 18 h) or FK866 (200 nM, 24 h). *; $p<0.05$,; $p<0.005$, ***; $p<0.0005$.**

inflammatory stroma and cellular senescence [41]. Recent reports have emphasized that low oxygen tension promotes and maintains the undifferentiated state of the stem cells [42–43]. In that sense, it is conceivable that response to damage exerted by hypoxia, acidosis or oxidative stress, which all occur in the tumor microenvironment, all favor cancer cell adaptation via increasing cell plasticity. This idea appears to be also applicable to normal cells as evidenced by a recent report showing that airway epithelial cells undergo dedifferentiation and convert into functional stem cells in response to the genotoxic drug, doxycycline [20]. Furthermore, the expression of *OCT4* and *NANOG* was shown in adipose tissue-derived stromal cells, which were maintained under hypoxic conditions (2% O_2) for over a span of 6 weeks [44].

The generation of spheres/mammospheres from single cells under non-adherent conditions in selective media is a widely used approach for enrichment of stem-like cells from cell lines and primary tumors. The spheroidal colonies were mostly generated on low adhesion plates by cells that were maintained in a serum free medium containing EGF and/or bFGF at 10–20 ng/ml supplemented with insulin, hydrocortisone and B27, which serves as a serum replacement. Using this approach, spheroidal colonies were generated from various primary cancers and cell lines such as T47D-C42, MCF7, MDA-MB231, MDA-MB468, BT474, and others [45–46]. However, no more than 3% of cells in spheroids were positive for aldehyde dehydrogenase-1 (ALDH), which was used to identify CSC. It should be pointed out that ALDH is also indicator of damage since it serves to mitigate cellular oxidative stress. While most cells from breast duct cells die under such conditions, a small number of cells survive which generate floating spheroidal colonies [47]. Similarly, spheroids isolated from primary ovarian cancer specimens show increased ALDH activity [48]. Data provided here suggest that spheroid cells with stem cell-like properties are generated in tumor cells that recover from any damage such as that induced by hypoxia, glucose deprivation, or acidosis, which all occur in the tumor microenvironment. Recently, Pease J.C and colleagues demonstrated spheroid formation in dense regions of cultures from four ovarian cancer cell lines [49]. Spheroid budding from monolayer correlated with epithelial to mesenchymal transition and led to drug resistance. However, dissociation of spheroids into a monolayer fully restored their drug sensitivity. Here, we show that cells that recover from damage, have elevated levels of H_2S and maintain a long term tolerance not only to depletion of nutrients but also show resistance to damage induced by drugs that are used in the treatment of cancer including bleomycin and cisplatin. It was shown that drug resistance is directly proportional to tumor size [50]. Consistent with this, our recently reported findings demonstrated that DR cells inoculated to immunodeficient mice formed larger tumors than those produced by Pc cells within

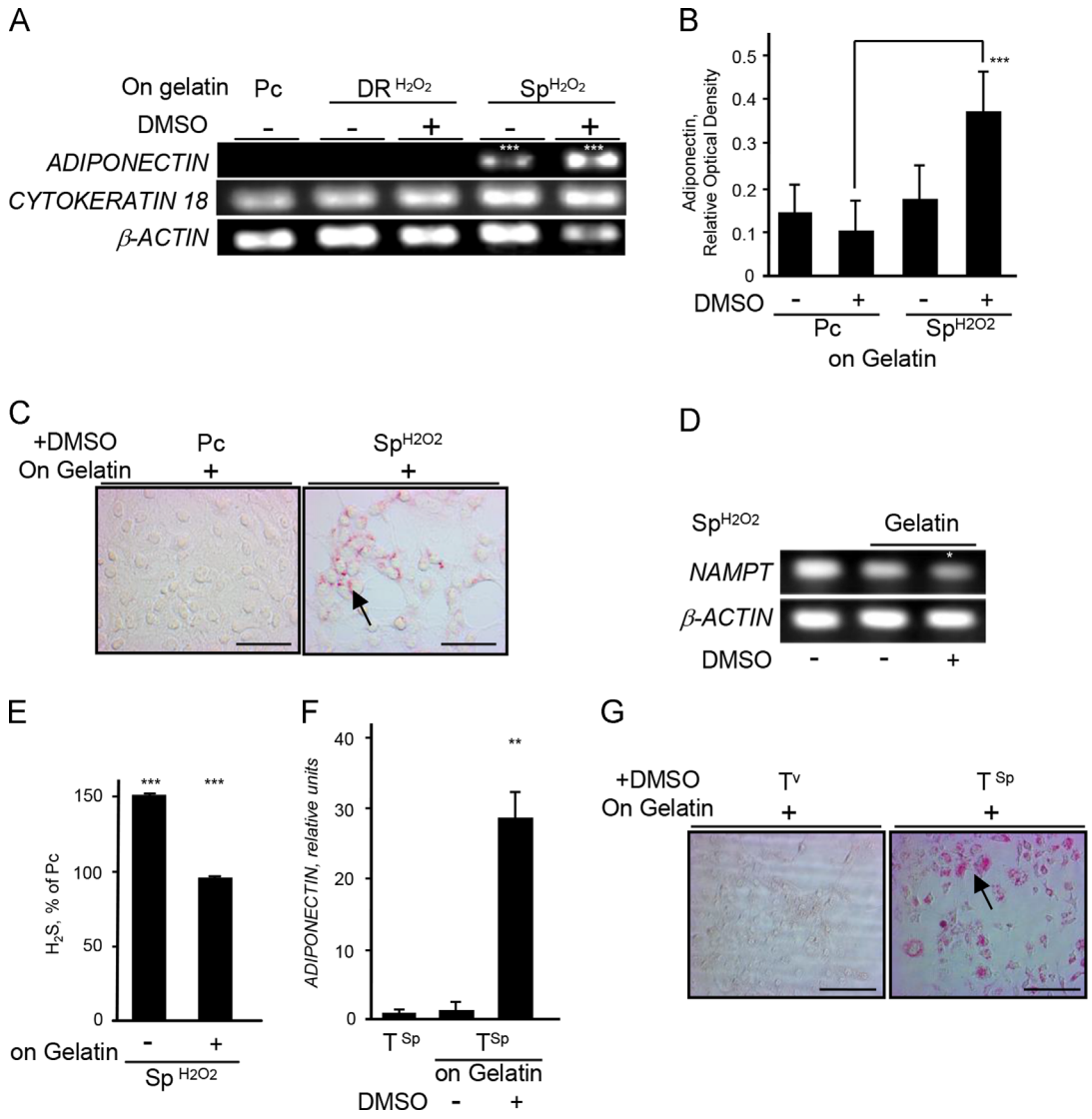

Fig. 8 – Spheroid cells from HepG2 tumor cells recovering from potentially lethal damage and cancer cells isolated from *in vivo* generated HepG2 tumors show adipogenic plasticity. Sp cells were cultured on 2% gelatin as ECM in the absence (−) and presence (+) of 1% DMSO for 5 days. A. The expression of *ADIPONECTIN* and *CYTOKERATIN 18* was assessed by RT-PCR analysis in Pc, DR^{H2O2} and Sp^{H2O2} cells. B. Relative level of *ADIPONECTIN* gene expression normalized to *β-ACTIN* in Pc and Sp^{H2O2} cells. C. Oil-Red-O staining of Pc and Sp^{H2O2} cells. Arrows point to Oil-Red-O positive cells. Scale bars, 50 μM. D. The expression of *NAMPT* in Sp^{H2O2} cells was assessed by RT-PCR analysis. E. H_2S production in 3D Sp^{H2O2} cells cultured on with (+) or without (−) 2% gelatin. F. Expression level of *ADIPONECTIN* assessed by real time PCR in 3D T^{Sp} cells and T^{Sp}. G. Oil-Red-O staining of HepG2 Tv and T^{Sp} cells isolated from *in vivo* generated tumors. Scale bars, 50 μM. **; $p<0.005$, *; $p<0.0005$.**

the same time frame [32]. These data indicate that DR cells which show increased drug resistance associated with expression of stem cell markers are more tumorigenic as compared to their parental counterpart cells. Cell dedifferentiation contributes to proliferation rate. Thus, *SOX2* overexpression alone is sufficient to drive cell proliferation by facilitating G1/S transition, whereas conditional deletion of *SOX2* was shown to decrease tumor formation after chemical-induced carcinogenesis [51–52].

Following recovery from damage, cancer cells of different lineages are stimulated to dedifferentiate. The results suggest that cancer cell phenotype is dynamic and stemness may be acquired through dedifferentiation following recovery from damage. The ability of cancer cells to acquire stem-specific gene expression and to transdifferentiate was proportional to the amount of H_2S and Nampt mediated increase in NAD^+. Consistent with this, inhibition of H_2S producing enzymes, their inhibitor, PAG, [53] significantly diminished the ability of cells to undergo dedifferentiation. In part, hydrogen sulfide exerts its effects by reducing the intracellular redox environment that favors the transition into an undifferentiated state. This is not surprising since H_2S was shown to ameliorate hypoxic and oxidative stress induced injury due to its ability to scavenge oxidative species and to increase the pool of reduced glutathione [54–58]. Tumor cells that survive acidic conditions demonstrate increased tolerance to damage and become dependent on low pH for prolonged survival [59]. H_2S is a weak acid and readily ionizes in aqueous solutions. At physiological pH, approximately 70% of total H_2S exists in anionic form as HS^-,

whereas under an acidic environment (pH 6) it is present in H_2S form [60]. The increase in amount of H_2S has an impact on total level of thiols and is associated with an increased cytoprotection. Thus, cytoprotective effectiveness of H_2S and its ability to promote the dedifferentiation might be dependent on microenvironmental conditions. Consistent with our observations, stem cells reside in niches which are characterized by a reduced redox state, critical for maintaining stemness, whereas oxidizing redox state promotes their differentiation [61–62]. Furthermore, the effect of H_2S on expression of stem cell markers is attributable to its ability to upregulate Nampt and, therefore, to the increase intracellular availability of NAD^+. This idea is supported by the finding that suppression of Nampt by its specific inhibitor, FK866, abrogates the expression of genes associated with an undifferentiated state. Nampt protein is overexpressed in multiple cancers and its inhibition suppresses the tumor growth. It was shown that inhibitors of Nampt prevent tumor spheroid formation, which is indicative of ability of single primary tumor cells to expand and repopulate tumors [63]. Nampt exerts its effects via regulation of level of NAD^+. Similar to our results, it was shown that upon depletion of NAD^+, human induced pluripotent cells lose their ability to remain undifferentiated [64]. The relative concentration of NAD^+ and NADH can be interconversed via oxidation/reduction reactions. However, only NADH can be significantly altered. Since oxygen is the final acceptor of reducing equivalent transferred by NADH, low oxygen tension results in an elevated NADH content. Increase in reduced NADH also indicates a shift in the intracellular redox state towards a more reducing environment.

Our results indicate that cancer cells that recover from damage induced by hypoxia or oxidative stress, and which express stem cell markers, also harbor the potential to transdifferentiate into new lineages underscoring development of new potencies. Although DMSO generally has an inhibitory effect on adipocyte differentiation in 3T3 L1 fibroblasts and 3T3 T mesenchymal stem cells [65], we have found that it promotes adipogenic differentiation of some damage recovered cancer cells. Adipogenic transdifferentiation may contribute to metabolic changes and affect tumor microenvironment. Upon adipogenic differentiation, mesenchymal stem cells were shown to acquire higher oxygen consumption and higher rates of reactive oxygen production which is indicative of a shift in redox environment to a more oxidized state [66]. Despite the high levels of mitochondrial respiration, differentiating mesenchymal stem cells were characterized by low ATP production and mitochondrial membrane potential. It is possible that at early stages of adipogenesis, a decrease in *NAMPT* expression might be the cause of a bioenergetic shortage. We show that transformation of tumor spheroid cells into cells showing an adipocytic phenotype was associated with a decrease in the expression of *NAMPT* and low production of H_2S. Consistent with our data, the knockdown of *NAMPT* or its direct inhibition by FK866 was shown to increase adipocyte formation in the mouse mesenchymal cell line C3H10T1/2 and in primary bone marrow stromal cells [67]. Furthermore, hypoxia was reported to inhibit adipogenic differentiation [66]. This evidence may explain the underlying cause for the inability of the spheroid cells recovered from hypoxia to transdifferentiate towards the adipogenic lineage. Li *et. al.* showed that during osteogenic differentiation of the multipotent mouse fibroblast, C3H10T1/2, and the omnipotent preosteoblast MC3T3-E1 cells, increase in *NAMPT* expression is followed by a rise in intracellular NAD^+ [68]. However, the authors show that early, during differentiation stage (on day 3), the expression level of *NAMPT* was not changed in MC3T3-E1 cells. We speculate that the observed difference in transdifferentiation potential between Sp cells generated from damage recovered HepG2 (ER^+) cells and MDA-MB-231 and MDA-MB-435 (ER^-) cells might be attributable to the status of estrogen receptor in these cells. Estrogen-related receptor-α (ERRα) has been reported to have a positive regulatory role in adipocytic differentiation, whereas cells deficient in ERRalpha were shown to display osteoblastic differentiation and mineralization [69–70]. It was reported that the plasticity shown towards osteogenesis and adipogenesis of human mesenchymal stem cells extend into osteogenic differentiation pathway with few cells still displaying adipogenic markers [71]. Moreover, it was recently shown that in bone marrow mesenchymal stem cells, H_2S regulates both self-renewal and osteogenic differentiation [72]. These findings suggest that the effect of H_2S on transdifferentiation might be contextual and might differ in cells of different lineages.

Taken together, data presented here suggest that H_2S–Nampt circuit plays an important role in cell fate determination. Upregulation of *ADPONECTIN* gene expression shows the ability of damage recovered cancer cells that form spheroids to transdifferentiate. Such a transdifferentiation potential is significant since it has been shown that adiponectin increases cell survival in glucose deprived colorectal cancer cells through enhancement of an autophagic response and induction of tumor vascularization in mammary cancers [73–74]. Full understanding of potential of cancer cells to dedifferentiate upon recovery from damage and the potency to transdifferentiate and to transform to new phenotypes has diverse implications in tumor cell biology.

Author contributions

RA, EO, SA designed and performed experiments and carried data analysis, SG reviewed and edited manuscript, ST designed experiments, carried data analysis, wrote and edited the manuscript.

The authors declare no competing financial interests or conflict of interests.

Acknowledgment

We thank to Dr. Michael D. Pluth for the generous gift of H_2S probe, HSN_2.

Appendix A. Supporting information

Supplementary data associated with this article can be found in the online version at http://dx.doi.org/10.1016/j.yexcr.2014.09.027.

REFERENCES

[1] P.B. Gupta, C.L. Chaffer, R.A. Weinberg, Cancer stem cells: mirage or reality? Nat. Med. 15 (2009) 1010–1012.
[2] F. Yuan, W. Zhou, C. Zou, Z. Zhang, H. Hu, Z. Dai, Y. Zhang, Expression of Oct4 in HCC and modulation to wnt/beta-catenin and TGF-beta signal pathways, Mol. Cell. Biochem. 343 (1-2) (2010) 155–162, http://dx.doi.org/10.1007/s11010-010-0509-3.
[3] Y.D. Wang, N. Cai, X.L. Wu, H.Z. Cao, L.L. Xie, P.S. Zheng, OCT4 promotes tumorigenesis and inhibits apoptosis of cervical cancer

cells by miR-125b/BAK1 pathway, Cell Death Dis. 8 (4) (2013) e760, http://dx.doi.org/10.1038/cddis.2013.272.
[4] Z. Chen, W.R. Xu, H. Qian, W. Zhu, X.F. Bu, S. Wang, S. Wang, Y.M. Yan, F. Mao, H.B. Gu, H.L. Cao, X.J. Xu, Oct4, a novel marker for human gastric cancer, J. Surg. Oncol. 99 (2009) 414–419, http://dx.doi.org/10.1002/jso.21270.
[5] T. Cantz, G. Key, M. Bleidissel, L. Gentile, D.W. Han, A. Brenne, H.R. Schöler, Absence of OCT4 expression in somatic tumor cell lines, Stem Cells 26 (3) (2008) 692–697.
[6] F. Wezel, J. Pearson, L.A. Kirkwood, J. Southgate, Differential expression of Oct4 variants and pseudogenes in normal urothelium and urothelial cancer, J. Am. J. Pathol. 183 (4) (2013) 1128–1136, http://dx.doi.org/10.1016/j.ajpath.2013.06.025.
[7] M. Herreros-Villanueva, J.S. Zhang, A.Koenig, E.V. Abel, T.C. Smyrk, W.R. Bamlet, A.A. de Narvajas, T.S. Gomez, D.M. Simeone, L. Bujanda, Billadeau D.D. SOX2 promotes dedifferentiation and imparts stem cell-like features to pancreatic cancer cells. Oncogenesis. 5, 2:e61. 10.1038/oncsis.2013.23. (2013).
[8] I. Dogan, S. Kawabata, E. Bergbower, J.J. Gills, A. Ekmekci, W. Wilson 3rd, C.M. Rudin, P.A. Dennis, SOX2 expression is an early event in a murine model of EGFR mutant lung cancer and promotes proliferation of a subset of EGFR mutant lung adenocarcinoma cell lines, Lung Cancer . (2014)http://dx.doi.org/10.1016/j.lungcan.2014.03.021 (Mar 29. pii: S0169-5002(14)00142-1).
[9] S. Amini, F. Fathi, J. Mobalegi, H. Sofimajidpour, T. Ghadimi, The expressions of stem cell markers: Oct4, Nanog, Sox2, nucleostemin, Bmi, Zfx, Tcl1, Tbx3, Dppa4, and Esrrb in bladder, colon, and prostate cancer, and certain cancer cell lines, Anat. Cell Biol. 47 (1) (2014) 1–11, http://dx.doi.org/10.5115/acb.2014.47.1.1.
[10] R. Wang, W. Liu, C.M. Helfer, J.E. Bradner, J.L. Hornick, S.M. Janicki, C.A. French, J. You, Activation of SOX2 expression by BRD4-NUT oncogenic fusion drives neoplastic transformation in NUT midline carcinoma, Cancer Res. (2014) (2014 Apr 16).
[11] A.D. Berezovsky, L.M. Poisson, D. Cherba, C.P. Webb, A.D. Transou, N.W. Lemke, X. Hong, L.A. Hasselbach, S.M. Irtenkauf, T. Mikkelsen, A.C. Decarvalho, Sox2 promotes malignancy in glioblastoma by regulating plasticity and astrocytic differentiation, Neoplasia 16 (3) . (2014)http://dx.doi.org/10.1016/j.neo.2014.03.006 (193-206.e25).
[12] P.Y. Tung, N.V. Varlakhanova, P.S. Knoepfler, Identification of DPPA4 and DPPA2 as a novel family of pluripotency-related oncogenes, Stem Cells 31 (11) (2013) 2330–2342, http://dx.doi.org/10.1002/stem.1526.
[13] N.E. Tchabo, P. Mhawech-Fauceglia, O.L. Caballero, J. Villella, A.F. Beck, A.J. Miliotto, J. Liao, C. Andrews, S. Lele, L.J. Old, K. Odunsi, Expression and serum immunoreactivity of developmentally restricted differentiation antigens in epithelial ovarian cancer, Cancer Immun. 26 (9) (2009) 6.
[14] L. Vermeulen, E. De Sousa, F. Melo, M. van der Heijden, K. Cameron, J.H. de Jong, T. Borovski, J.B. Tuynman, M. Todaro, C. Merz, H. Rodermond, M.R. Sprick, K. Kemper, D.J. Richel, G. Stassi, J.P. Medema, Wnt activity defines colon cancer stem cells and is regulated by the microenvironment, Nat. Cell Biol. 12 (5) (2010) 468–476, http://dx.doi.org/10.1038/ncb2048.
[15] S.A. Mani, W. Guo, M.J. Liao, E.N. Eaton, A. Ayyanan, A.Y. Zhou, M. Brooks, F. Reinhard, C.C. Zhang, M. Shipitsin, L.L. Campbell, K. Polyak, C. Brisken, J. Yang, R.A. Weinberg, The epithelial-mesenchymal transition generates cells with properties of stem cells, Cell 133 (4) (2008) 704–715, http://dx.doi.org/10.1016/j.cell.2008.03.027 (16).
[16] M.J. Liao, C.C. Zhang, B. Zhou, D.B. Zimonjic, S.A. Mani, M. Kaba, A. Gifford, F. Reinhardt, N.C. Popescu, W. Guo, E.N. Eaton, H.F. Lodish, R.A. Weinberg, Enrichment of a population of mammary gland cells that form mammospheres and have in vivo repopulating activity, Cancer Res. 67 (17) (2007) 8131–8138.
[17] Y. Wang, J. Yang, H. Zheng, G.J. Tomasek, P. Zhang, P.E. McKeever, E.Y. Lee, Y. Zhu, Expression of mutant p53 proteins implicates a lineage relationship between neural stem cells and malignant astrocytic glioma in a murine model, Cancer Cell 15 (2009) 514–526.
[18] M.F. Clarke, J.E. Dick, P.B. Dirks, C.J. Eaves, C.H. Jamieson, D.L. Jones, J. Visvader, I.L. Weissman, G.M. Wahl, Cancer stem cells–perspectives on current status and future directions: AACR Workshop on cancer stem cells, Cancer Res. 66 (2006) 9339–9344.
[19] S. Schwitalla, A.A. Fingerle, P. Cammareri, T. Nebelsiek, S.I. Göktuna, P.K. Ziegler, O. Canli, J. Heijmans, D.J. Huels, G. Moreaux, R.A. Rupec, M. Gerhard, R. Schmid, N. Barker, H. Clevers, R. Lang, J. Neumann, T. Kirchner, M.M. Taketo, G.R. van den Brink, O.J. Sansom, M.C. Arkan, F.R. Greten, Intestinal tumorigenesis initiated by dedifferentiation and acquisition of stem-cell-like properties, Cell 152 (1-2) (2013) 25–38, http://dx.doi.org/10.1016/j.cell.2012.12.012.
[20] P.R. Tata, H. Mou, A. Pardo-Saganta, R. Zhao, M. Prabhu, B.M. Law, V. Vinarsky, J.L. Cho, S. Breton, A. Sahay, B.D. Medoff, J. Rajagopal, Dedifferentiation of committed epithelial cells into stem cells in vivo, Nature 503 (7475) (2013) 218–223, http://dx.doi.org/10.1038/nature12777.
[21] D.P. Heller, M.M. Feeley, G.P. Raaphorst, Changes in survival and potentially lethal damage recovery following periods of high and low metabolic activity in human glioma cells, Oncol. Res. 5 (1993) 475–482.
[22] M.E. Varnes, L.A. Dethlefsen, J.E. Biaglow, The effect of pH on potentially lethal damage recovery in A549 cells, Radiat. Res. 108 (1986) 80–90.
[23] J. Midander, P.J. Deschavanne, D. Debieu, E.P. Malaise, L. Revesz, Reduced repair of potentially lethal radiation damage in glutathione synthetase-deficient human fibroblasts after X-irradiation, Int. J. Radiat. Biol. Relat. Stud. Phys. Chem. Med. 49 (3) (1986) 403–413.
[24] Y. Kimura, H. Kimura, Hydrogen sulfide protects neurons from oxidative stress, FASEB J. 18 (10) (2004) 1165–1167.
[25] M.H. Stipanuk, Sulfur amino acid metabolism: pathways for production and removal of homocysteine and cysteine, Annu. Rev. Nutr. 24 (2004) 539–577.
[26] S. Singh, D. Padovani, R.A. Leslie, T. Chiku, R. Banerjee, Relative contributions of cystathionine beta-synthase and gamma-cystathionase to H_2S biogenesis via alternative trans-sulfuration reactions, J. Biol. Chem. 284 (2009) 22457–22466, http://dx.doi.org/10.1074/jbc.M109.010868.
[27] A. Meister, P.E. Fraser, S.V. Tice, Enzymatic desulfuration of beta-mercaptopyruvate to pyruvate, J. Biol. Chem. 206 (1954) 561–575.
[28] N. Shibuya, Y. Mikami, Y. Kimura, N. Nagahara, H. Kimura, Vascular endothelium expresses 3-mercaptopyruvate sulfurtransferase and produces hydrogen sulfide, J. Biochem. 146 (2009) 623–626, http://dx.doi.org/10.1093/jb/mvp111.
[29] J.C. Mathai, A. Missner, P. Kügler, S.M. Saparov, M.L. Zeidel, J.K. Lee, P. Pohl, No facilitator required for membrane transport of hydrogen sulfide, Proc. Natl. Acad. Sci. USA 106 (39) (2009) 16633–16638, http://dx.doi.org/10.1073/pnas.0902952106.
[30] A. Fago, F.B. Jensen, B. Tota, M. Feelisch, K.R. Olson, S. Helbo, S. Lefevre, D. Mancardi, A. Palumbo, G.K. Sandvik, N. Skovgaard, Integrating nitric oxide, nitrite and hydrogen sulfide signaling in the physiological adaptations to hypoxia: a comparative approach, Comp. Biochem. Physiol. A Mol. Integr. Physiol. 162 (1) (2012) 1–6, http://dx.doi.org/10.1016/j.cbpa.2012.01.011.
[31] X.B. Dong, C.T. Yang, D.D. Zheng, L.Q. Mo, X.Y. Wang, A.P. Lan, F. Hu, P.X. Chen, J.Q. Feng, M.F. Zhang, X.X. Liao, Inhibition of ROS-activated ERK1/2 pathway contributes to the protection of H_2S against chemical hypoxia-induced injury in H9c2 cells, Mol. Cell Biochem. 362 (1-2) (2012) 149–157, http://dx.doi.org/10.1007/s11010-011-1137-2.
[32] S. Akakura, E. Ostrakhovitch, R. Sanokawa-Akakura, S. Tabibzadeh, Cancer cells recovering from damage exhibit mitochondrial

restructuring and increased aerobic glycolysis, Biochem. Biophys. Res. Commun. 488 (2014) 461–466.
[33] T.P. Szatrowski, C.F. Nathan, Production of large amounts of hydrogen peroxide by human tumor cells, Cancer Res. 51 (3) (1991) 794–798.
[34] O. Fernandez-Capetillo, S.K. Mahadevaiah, A. Celeste, P.J. Romanienko, R.D. Camerini-Otero, W.M. Bonner, K. Manova, P. Burgoyne, A. Nussenzweig, H2AX is required for chromatin remodeling and inactivation of sex chromosomes in male mouse meiosis, Dev. Cell. 4 (2003) 497–508.
[35] L.A. Montoya, M.D. Pluth, Selective turn-on fluorescent probes for imaging hydrogen sulfide in living cells, Chem. Commun. (Camb) 48 (39) (2012) 4767–4769, http://dx.doi.org/10.1039/c2cc30730h.
[36] E.J. Norris, C.R. Culberson, S. Narasimhan, M.G. Clemens, The liver as a central regulator of hydrogen sulfide, Shock 36 (3) (2011) 242–250, http://dx.doi.org/10.1097/SHK.0b013e3182252ee7.
[37] Y. Gao, J. Wei, J. Han, X. Wang, G. Su, Y. Zhao, B. Chen, Z. Xiao, J. Cao, J. Dai, The novel function of OCT4B isoform-265 in genotoxic stress, Stem Cells 30 (4) (2012) 665–672, http://dx.doi.org/10.1002/stem.1034.
[38] M. Jez, S. Ambady, O. Kashpur, A. Grella, C. Malcuit, L. Vilner, P. Rozman, T. Dominko, Expression and differentiation between OCT4A and its Pseudogenes in human ESCs and differentiated adult somatic cells, PLoS One 9 (2) (2014) e89546, http://dx.doi.org/10.1371/journal.pone.0089546.
[39] M.D. O'Connor, M.D. Kardel, I. Iosfina, D. Youssef, M. Lu, M.M. Li, S. Vercauteren, A. Nagy, C.J. Eaves, Alkaline phosphatase-positive colony formation is a sensitive, specific, and quantitative indicator of undifferentiated human embryonic stem cells, Stem Cells 26 (5) (2008) 1109–1116, http://dx.doi.org/10.1634/stemcells.2007-0801.
[40] T. Redmer, S. Diecke, T. Grigoryan, A. Quiroga-Negreira, W. Birchmeier, D. Besser, E-cadherin is crucial for embryonic stem cell pluripotency and can replace OCT4 during somatic cell reprogramming, EMBO Rep. 12 (7) (2011) 720–726, http://dx.doi.org/10.1038/embor.2011.88.
[41] P. Csermely, J. Hódsági, T. Korcsmáros, D. Módos, A.R. Perez-Lopez, K. Szalay, D.V. Veres, K. Lenti, L.Y. Wu, X.S. Zhang, Cancer stem cells display extremely large evolvability: alternating plastic and rigid networks as a potential mechanism: network models, novel therapeutic target strategies, and the contributions of hypoxia, inflammation and cellular senescence, Semin. Cancer Biol. pii: S1044-579X(13)00130-2 . (2014)http://dx.doi.org/10.1016/j.semcancer.2013.12.004.
[42] A. Mohyeldin, T. Garzon-Muvdi, A. Quinones-Hinojosa, Oxygen in stem cell biology: a critical component of the stem cell niche, Cell Stem Cell 7 (2) (2010) 150–161, http://dx.doi.org/10.1016/j.stem.2010.07.007.
[43] Y. Yoshida, K. Takahashi, K. Okita, T. Ichisaka, S. Yamanaka, Hypoxia enhances the generation of induced pluripotent stem cells, Cell Stem Cell 5 (3) (2009) 237–241, http://dx.doi.org/10.1016/j.stem.2009.08.001.
[44] Y. Yamamoto, M. Fujita, Y. Tanaka, I. Kojima, Y. Kanatani, M. Ishihara, S. Tachibana, Low oxygen tension enhances proliferation and maintains stemness of adipose tissue-derived stromal cells, Biores. Open Access 2 (3) (2013) 199–205, http://dx.doi.org/10.1089/biores.2013.0004.
[45] P. Grudzien, S. Lo, K.S. Albain, P. Robinson, P. Rajan, P.R. Strack, T.E. Golde, L. Miele, K.E. Foreman, Inhibition of Notch signaling reduces the stem-like population of breast cancer cells and prevents mammosphere formation, Anticancer Res. 30 (10) (2010) 3853–3867.
[46] G. Farnie, R.B. Clarke, K. Spence, N. Pinnock, K. Brennan, N.G. Anderson, N.J. Bundred, Novel cell culture technique for primary ductal carcinoma in situ: role of Notch and epidermal growth factor receptor signaling pathways, J. Natl. Cancer Inst. 99 (8) (2007) 616–627.
[47] G. Dontu, W.M. Abdallah, J.M. Foley, K.W. Jackson, M.F. Clarke, M.J. Kawamura, M.S. Wicha, In vitro propagation and transcriptional profiling of human mammary stem/progenitor cells, Genes Dev. 17 (10) (2003) 1253–1270.
[48] J. Liao, F. Qian, N. Tchabo, P. Mhawech-Fauceglia, A. Beck, Z. Qian, X. Wang, W.J. Huss, S.B. Lele, C.D. Morrison, K. Odunsi, Ovarian cancer spheroid cells with stem cell-like properties contribute to tumor generation, metastasis and chemotherapy resistance through hypoxia-resistant metabolism, PLoS One 9 (1) (2014) e84941, http://dx.doi.org/10.1371/journal.pone.0084941.
[49] J.C. Pease, M. Brewer, J.S. Tirnauer, Spontaneous spheroid budding from monolayers: a potential contribution to ovarian cancer dissemination, Biol. Open 1 (7) (2012) 622–628, http://dx.doi.org/10.1242/bio.2012653.
[50] P. Wachsberger, R. Burd, A.P. Dicker, Tumor response to ionizing radiation combined with antiangiogenesis or vascular targeting agents: exploring mechanisms of interaction, Clin. Cancer Res. 9 (6) (2003) 1957–1971.
[51] M. Herreros-Villanueva, J.S. Zhang, A. Koenig, E.V. Abel, T.C. Smyrk, W.R. Bamlet, A.A. de Narvajas, T.S. Gomez, D.M. Simeone, L. Bujanda, D.D. Billadeau, SOX_2 promotes dedifferentiation and imparts stem cell-like features to pancreatic cancer cells, Oncogenesis 2 (2013) e61, http://dx.doi.org/10.1038/oncsis.2013.23.
[52] S. Boumahdi, G. Driessens, G. Lapouge, S. Rorive, D. Nassar, M. Le Mercier, B. Delatte, A. Caauwe, S. Lenglez, E. Nkusi, S. Brohée, I. Salmon, C. Dubois, V. del Marmol, F. Fuks, B. Beck, C. Blanpain, SOX_2 controls tumour initiation and cancer stem-cell functions in squamous-cell carcinoma, Nature 511 (7508) (2014) 246–250, http://dx.doi.org/10.1038/nature13305.
[53] K. Abe, H. Kimura, The possible role of hydrogen sulfide as an endogenous neuromodulator, J. Neurosci. 16 (3) (1996) 1066–1071.
[54] D.P. Jones, Redefining oxidative stress, Antioxid. Redox Signal. 8 (2006) 1865–1879.
[55] M.Y. Ali, C.Y. Ping, Y.Y. Mok, L. Ling, M. Whiteman, M. Bhatia, P. Moore, Regulation of vascular nitric oxide in vitro and in vivo; a new role for endogenous hydrogen sulphide?, Br. J. Pharm. 149 (2006) 625–634.
[56] S. Muzaffar, N. Shukla, M. Bond, A.C. Newby, G.D. Angelini, A. Sparatore, P. Del Soldato, J.Y. Jeremy, Exogenous hydrogen sulfide inhibits superoxide formation, NOX-1 expression and Rac1 activity in human vascular smooth muscle cells, J. Vasc. Res. 45 (2008) 521–528, http://dx.doi.org/10.1159/000129686.
[57] Y.Y. Liu, B.V. Nagpure, P.T. Wong, J.S. Bian, Hydrogen sulfide protects SH-SY5Y neuronal cells against d-galactose induced cell injury by suppression of advanced glycation end products formation and oxidative stress, Neurochem. Int. 62 (5) (2013) 603–609, http://dx.doi.org/10.1016/j.neuint.2012.12.010.
[58] Z.W. Lee, Y.L. Low, S. Huang, T. Wang, L.W. Deng, Cystathionine-γ-lyase/hydrogen sulfide system maintains cellular glutathione status, Biochem. J. (2014).
[59] J.W. Wojtkowiak, J.M. Rothberg, V. Kumar, K.J. Schramm, E. Haller, J.B. Proemsey, M.C. Lloyd, B.F. Sloane, R.J. Gillies, Chronic autophagy is a cellular adaptation to tumor acidic pH microenvironments, Cancer Res. 72 (2012) 3938–3947, http://dx.doi.org/10.1158/0008-5472.CAN-11-3881.
[60] J.P. Hershey, T. Plese, F.J. Miller, The pK1 for the dissociation of H_2S in various ionic media, Geo- Chim. et Cosmochimica Acta 52 (1988) 2047–2051.
[61] S. Pervaiz, R. Taneja, S. Ghaffari, Oxidative stress regulation of stem and progenitor cells, Antioxid. Redox Signal. 11 (2009) 2777–2789, http://dx.doi.org/10.1089/ars.2009.2804.
[62] X. Shi, Y. Zhang, J. Zheng, J. Pan, Reactive oxygen species in cancer stem cells, Antioxid. Redox Signal. 16 (2012) 1215–1228, http://dx.doi.org/10.1089/ars.2012.4529.

[63] Y. Luo, C. Yang, M. Ye, C. Jin, J.L. Abbruzzese, M.H. Lee, S.C. Yeung, W.L. McKeehan, Deficiency of metabolic regulator FGFR4 delays breast cancer progression through systemic and microenvironmental metabolic alterations, Cancer Metab. 1 (1) . (2013)http://dx.doi.org/10.1186/2049-3002-1-21 (21).
[64] M.J. Son, M.Y. Son, B. Seol, M.J. Kim, C.H. Yoo, M.K. Han, Y.S. Cho, Nicotinamide overcomes pluripotency deficits and reprogramming barriers, Stem Cells 31 (6) (2013) 1121–1135, http://dx.doi.org/10.1002/stem.1368.
[65] H. Wang, R.E. Scott, Inhibition of distinct steps in the adipocyte differentiation pathway in 3T3 T mesenchymal stem cells by dimethyl sulphoxide (DMSO), Cell Prolif. 26 (1) (1993) 55–66.
[66] Y. Zhang, G. Marsboom, P.T. Toth, J. Rehman, Mitochondrial respiration regulates adipogenic differentiation of human mesenchymal stem cells, PLoS One 8 (10) (2013) e77077, http://dx.doi.org/10.1371/journal.pone.0077077.
[67] Y. Li, X. He, Y. Li, J. He, B. Anderstam, G. Andersson, U. Lindgren, Nicotinamide phosphoribosyltransferase (Nampt) affects the lineage fate determination of mesenchymal stem cells: a possible cause for reduced osteogenesis and increased adipogenesis in older individuals, J. Bone Miner. Res. 26 (11) (2011) 2656–2664, http://dx.doi.org/10.1002/jbmr.480.
[68] Y. Li, J. He, X. He, Y. Li, U. Lindgren, Nampt expression increases during osteogenic differentiation of multi- and omnipotent progenitors, Biochem. Biophys. Res. Commun. 434 (1) (2013) 117–123, http://dx.doi.org/10.1016/j.bbrc.2013.02.132.
[69] A.M. Rajalin, H. Pollock, P. Aarnisalo, ERRalpha regulates osteoblastic and adipogenic differentiation of mouse bone marrow mesenchymal stem cells, Biochem. Biophys. Res. Commun. 396 (2) (2010) 477–482, http://dx.doi.org/10.1016/j.bbrc.2010.04.120.
[70] D. Ju, J. He, L. Zhao, X. Zheng, G. Yang, Estrogen related receptor α-induced adipogenesis is PGC-1β-dependent, Mol. Biol. Rep. 39 (3) (2012) 3343–3354, http://dx.doi.org/10.1007/s11033-011-1104-8.
[71] T. Schilling, U. Nöth, L. Klein-Hitpass, F. Jakob, N. Schütze, Plasticity in adipogenesis and osteogenesis of human mesenchymal stem cells, Mol. Cell. Endocrinol. 271 (1-2) (2007) 1–17.
[72] Y. Liu, R. Yang, X. Liu, Y. Zhou, C. Qu, T. Kikuiri, S. Wang, E. Zandi, J. Du, I.S. Ambudkar, S. Shi, Hydrogen sulfide maintains mesenchymal stem cell function and bone homeostasis via regulation of Ca^{2+} channel sulfhydration, Cell Stem Cell . (2014) http://dx.doi.org/10.1016/j.stem.2014.03.005.
[73] B.S. Habeeb, J. Kitayama, H. Nagawa, Adiponectin supports cell survival in glucose deprivation through enhancement of autophagic response in colorectal cancer cells, Cancer Sci. 102 (5) (2011) 999–1006, http://dx.doi.org/10.1111/j.1349-7006.2011.01902.x.
[74] M.S. Denzel, L.W. Hebbard, G. Shostak, L. Shapiro, R.D. Cardiff, B. Ranscht, Adiponectin deficiency limits tumor vascularization in the MMTV-PyV-mT mouse model of mammary cancer, Clin. Cancer Res. 15 (10) (2009) 3256–3264, http://dx.doi.org/10.1158/1078-0432.CCR-08-2661.